




# Synthetic biology for improved hydrogen production in *Chlamydomonas reinhardtii*

Samuel J. King, Ante Jerkovic, Louise J. Brown,   
Kerstin Petroll\*\*  and Robert D. Willows\*   
Department of Molecular Sciences, Macquarie  
University, Sydney, NSW, Australia.

## Summary

Hydrogen is a clean alternative to fossil fuels. It has applications for electricity generation and transportation and is used for the manufacturing of ammonia and steel. However, today, H<sub>2</sub> is almost exclusively produced from coal and natural gas. As such, methods to produce H<sub>2</sub> that do not use fossil fuels need to be developed and adopted. The biological manufacturing of H<sub>2</sub> may be one promising solution as this process is clean and renewable. Hydrogen is produced biologically via enzymes called hydrogenases. There are three classes of hydrogenases namely [FeFe], [NiFe] and [Fe] hydrogenases. The [FeFe] hydrogenase HydA1 from the model unicellular algae *Chlamydomonas reinhardtii* has been studied extensively and belongs to the A1 subclass of [FeFe] hydrogenases that have the highest turnover frequencies amongst hydrogenases (21,000 ± 12,000 H<sub>2</sub> s<sup>-1</sup> for CaHydA from *Clostridium acetobutylicum*). Yet to date, limitations in *C. reinhardtii* H<sub>2</sub> production pathways have hampered commercial scale implementation, in part due to O<sub>2</sub> sensitivity of hydrogenases and competing metabolic pathways, resulting in low H<sub>2</sub> production efficiency. Here, we describe key processes in the biogenesis of HydA1 and H<sub>2</sub> production pathways in *C. reinhardtii*. We also summarize recent advancements of algal H<sub>2</sub>

production using synthetic biology and describe valuable tools such as high-throughput screening (HTS) assays to accelerate the process of engineering algae for commercial biological H<sub>2</sub> production.

## Introduction

Hydrogen is the most abundant element in the universe, but on earth, it mostly exists as compounds with other elements. Thus, molecular H<sub>2</sub> is not readily available and needs to be manufactured. Hydrogen has a high gravimetric energy density (~ 120 MJ kg<sup>-1</sup>), approximately triple that of gasoline (~ 46 MJ kg<sup>-1</sup>) (Ley *et al.*, 2014), and can be directly converted to electricity via a H<sub>2</sub> fuel cell, only emitting heat and water as local by-products (Wu *et al.*, 2012). Furthermore, H<sub>2</sub> is used for manufacturing of chemicals including the production of ammonia for fertilizer, for steel manufacturing, and also the methanol industry (Ramachandran and Menon, 1998). To date, commercially available H<sub>2</sub> is sourced primarily from fossil fuels with approximately 99% manufactured from coal (76%) and natural gas (23%), typically via coal gasification and steam reformation (IEA, 2019). As such, renewable and sustainable methods for H<sub>2</sub> production are required to decarbonize the H<sub>2</sub> economy.

One means to supply clean H<sub>2</sub> is through water electrolysis. However, the worldwide large scale electrolyser capacity is only sufficient to provide less than 0.1% of the current H<sub>2</sub> demand (IEA, 2019). Commercial electrolysers today also require highly purified water and typically must operate continuously, which is generally not compatible with intermittent electricity supply from solar and wind. While there is ongoing work to improve the efficiency and scale of electrolysis to be more economically viable (Burton *et al.*, 2021), other sustainable and low-carbon methods for producing renewable H<sub>2</sub> should also be examined to help accelerate the transition to achieving a renewable H<sub>2</sub> economy.

The field of microbial biotechnology has the potential to contribute to the production of carbon-neutral and renewable H<sub>2</sub>. Organisms from all 3 domains of life can produce H<sub>2</sub> using enzymes known as hydrogenases (Peters *et al.*, 2015). In general, hydrogenases catalyse

Received 24 November, 2021; revised 9 February, 2022; accepted 11 February, 2022.

For correspondence. \*E-mail robert.willows@mq.edu.au Tel. +61 2 9850 8146; Fax +61 2 9850 8313. \*\*E-mail kerstin.petroll@mq.edu.au; Tel. +61 2 9850 8219; Fax +61 2 9850 8313.

*Microbial Biotechnology* (2022) 15(7), 1946–1965  
doi:10.1111/1751-7915.14024

## Funding information

SK is supported by a Macquarie University RTP Scholarship. TJ and KP are supported by the Australian Renewable Energy Agency (ARENA) grant RW0003 awarded to RDW and LB.

© 2022 The Authors. *Microbial Biotechnology* published by Society for Applied Microbiology and John Wiley & Sons Ltd.

This is an open access article under the terms of the Creative Commons Attribution-NonCommercial License, which permits use, distribution and reproduction in any medium, provided the original work is properly cited and is not used for commercial purposes.

the reversible oxidation of protons into H<sub>2</sub>. There are three classes of hydrogenase: [Fe], [NiFe] and [FeFe]. These three classes can be further separated into 38 subclasses according to their biological function and substrates (Søndergaard *et al.*, 2016). The [Fe] hydrogenases are a unique case as they are only used by a select group of methanogenic archaea and function differently to [NiFe] and [FeFe] hydrogenases, splitting H<sub>2</sub> into H<sup>+</sup> and H<sup>-</sup> and delivering the hydride to methenyltetrahydromethanopterin (methenyl-H<sub>4</sub>MPT<sup>+</sup>) (Nicolet, 2019). Many similar functions are shared amongst the 29 [NiFe] subclasses and 8 [FeFe] subclasses such as H<sub>2</sub> evolution, H<sub>2</sub> oxidation, bifurcating H<sub>2</sub> evolution/oxidation, bidirectional H<sub>2</sub> evolution/oxidation and H<sub>2</sub>/H<sup>+</sup> sensory functions (Søndergaard *et al.*, 2016). Additionally, [NiFe] and [FeFe] hydrogenases have similar structures, both contain a di-metallic active centre bridged by sulfur (S) atoms with additional CO and CN ligands. Despite these similarities, the [NiFe] and [FeFe] hydrogenases do not share a common ancestor and seem to be a remarkable case of convergent evolution (Peters *et al.*, 2015).

From a biotechnological standpoint, [FeFe] and [NiFe] hydrogenases each have advantages and disadvantages. [FeFe] hydrogenases have the highest rates of H<sub>2</sub> production reported so far, with turnover frequencies as high as 21,000 ± 12,000 H<sub>2</sub> s<sup>-1</sup> for CaHydA from *Clostridium acetobutylicum* (Madden *et al.*, 2012). However, the [FeFe] hydrogenase class are extremely labile in the presence of O<sub>2</sub> with concentrations as low as 0.01% O<sub>2</sub> shown to damage the enzyme *in vitro* (Swanson *et al.*, 2015). In comparison, the [NiFe] hydrogenases display lower turnover frequencies, such as 1,340 ± 115 H<sub>2</sub> s<sup>-1</sup> for the hydrogenase produced by *Synechocystis* sp. PCC 6803 (Gutekunst *et al.*, 2018). However, approximately 44% of the ~2000 identified [NiFe] hydrogenases are predicted to be O<sub>2</sub> tolerant, which can be advantageous as maintaining strict anaerobic conditions is difficult at scale for commercial applications (Cracknell *et al.*, 2009; Søndergaard *et al.*, 2016). This review will focus on FeFe hydrogenases, specifically HydA1, and developments that improve their H<sub>2</sub> production.

Biological H<sub>2</sub> production catalysed by [FeFe] hydrogenases requires a characteristic cofactor known as the H-cluster, with a maturation system both forming and inserting the H-cluster cofactor into the [FeFe] hydrogenase. Components of this maturation system include the S utilization factor (SUF) iron-sulfur (Fe-S) assembly machinery in conjunction with the GTPase HydF and the radical SAM (rSAM) enzymes HydE and HydG. These components facilitate the stepwise biosynthesis and insertion of the H-cluster into [FeFe] hydrogenases.

One of the best-characterized [FeFe] hydrogenases is the [FeFe] hydrogenase HydA1 from *C. reinhardtii*. *C. reinhardtii* is a unicellular phototrophic green algae and a model organism, which has been studied extensively since the mid-20th century for fundamental processes such as photosynthesis and H<sub>2</sub> production (Sasso *et al.*, 2018). Phototrophic microalgae, like *C. reinhardtii*, are of great interest to the biotechnology industry since they can be grown to high densities in photobioreactors and harness solar energy for producing biomass and a wealth of valuable compounds, including H<sub>2</sub> (Fabris *et al.*, 2020). In *C. reinhardtii*, there are two endogenous [FeFe] hydrogenases capable of producing H<sub>2</sub>: HydA1 (accounting for ~80% of the total H<sub>2</sub> production) and HydA2 (accounting for ~20% of the total H<sub>2</sub> production) (Godman *et al.*, 2010; Meuser *et al.*, 2012). *C. reinhardtii* also contains a HydEF fusion protein that is analogous to the individual HydE and HydF proteins found in other organisms (Posewitz *et al.*, 2004a). Both HydA1 and HydA2 belong to the [FeFe] A1 subclass that evolves H<sub>2</sub> via oxidation of ferredoxins (Søndergaard *et al.*, 2016), which are Fe-S proteins that function as electron carriers in several important metabolic processes including H<sub>2</sub> production, nitrogen fixation and photosynthesis (Zanetti and Pandini, 2013). Specifically, HydA1 and HydA2 catalyse the reversible reduction in protons into H<sub>2</sub> either using energy from light (biophotolysis), or by oxidizing organic compounds such as starch (dark fermentation). Biophotolysis, the process of splitting water into H<sub>2</sub> and O<sub>2</sub>, is unique to green algae and cyanobacteria and is suggested to function as a transient electron sink for excess reductive energy when *C. reinhardtii* is transitioned from the dark to light under anoxic conditions. This rapid restoration of redox balance is essential for the onset of photosynthesis and CO<sub>2</sub> assimilation (Ghyssels *et al.*, 2013).

To successfully adopt *C. reinhardtii* H<sub>2</sub> production into industrial applications, several technical limitations must be overcome. A major limitation is the low efficiency of conversion of light to H<sub>2</sub> due to competition of the electrons with CO<sub>2</sub> fixation through the Calvin-Benson-Bassham (CBB) cycle. One of the highest reported efficiencies of light to H<sub>2</sub> conversion is only about 10% of the theoretical maximum (Kanygin *et al.*, 2020). Second, the rapid inactivation of [FeFe] hydrogenases by O<sub>2</sub> is a challenge limiting H<sub>2</sub> production, especially when considering that O<sub>2</sub> is also generated during the biophotolysis process. Hence, H<sub>2</sub> production in *C. reinhardtii* is generally a short-lived process lasting only a few minutes. The sustained production of H<sub>2</sub> can however be achieved over several days through the use of nutrient-deprived media supplemented with an organic carbon source (Sri-rangan *et al.*, 2011), or through implementation of tightly

controlled dark-light cycles (Kosourov *et al.*, 2018). However, both these solutions are not ideal for commercial scale-up processes as they are considered as non-ideal growth conditions. To overcome these limitations, the design-build-test-learn framework of synthetic biology can be applied to improving H<sub>2</sub> production by *C. reinhardtii* (Fig. 1).

The increased availability of sequenced genomes, as well as the development of new genetic tools in Synthetic Biology, is greatly facilitating the engineering of microorganisms for robust, biotechnological applications (Salomé and Merchant, 2019). Synthetic Biology is an emergent technology that simplifies and modularizes natural systems into standardized parts with distinct functions and defined design rules. By rationally combining novel or heterologous parts, altering existing systems and undertaking iterative design-build-test-learn cycles, the aim is to engineer new and better systems with specific outcomes and applications.

To date, many advances have been made in engineering microalgae such as *C. reinhardtii* for improved production of high-value compounds and biofuels including H<sub>2</sub> (Gimpel *et al.*, 2015; Jagadevan *et al.*, 2018; Fabris *et al.*, 2020; Ng *et al.*, 2020; Wichmann *et al.*, 2020). These advances include targeted recombinant protein expression in the chloroplast and nucleus using modularized toolkits (Lauersen *et al.*, 2015); development of several inducible and constitutive native and synthetic promoters (Fischer and Rochaix, 2001; Fei and Deng, 2007; Scranton *et al.*, 2016); editing tools such as precise gene editing through zinc-finger-nucleases technology and CRISPR/Cas9 technology (Shin *et al.*, 2016;

Greiner *et al.*, 2017; Guzmán-Zapata *et al.*, 2019); and miRNA gene silencing for metabolic engineering (Crozet *et al.*, 2018). Riboswitches, specific components of an mRNA molecule that regulate gene expression have also been used for metabolic engineering in the cyanobacterium *Synechococcus elongatus* and could be applied to *C. reinhardtii* (Nakahira *et al.*, 2013). In addition, new HTS tools are being developed to screen large algal strain libraries for superior traits, including for H<sub>2</sub> production (Schrader *et al.*, 2008; Stapleton and Swartz, 2010a, 2010b; Wecker and Ghirardi, 2014; Land *et al.*, 2019). Typically, knowledge about the organism, its genome, gene regulations, metabolic and signalling pathways can be of great benefit for the targeted design of improved traits and phenotypes.

Therefore, this review aimed to identify Synthetic Biology targets for improving H<sub>2</sub> production in *C. reinhardtii*, by summarizing current knowledge of HydA1-mediated H<sub>2</sub> production in *C. reinhardtii* holistically, including transcription, translation, transport, maturation and mechanistic limitations for H<sub>2</sub> production. We then highlight examples of how Synthetic Biology has been successfully used to alter and improve the native H<sub>2</sub> production system in *C. reinhardtii* and describe several available HTS assays that may help accelerate future screening of engineered *C. reinhardtii* for improved H<sub>2</sub> production.

### Biogenesis of HydA1

Many processes are involved in the biogenesis of HydA1 in *C. reinhardtii* including transcription, translation, transport into the chloroplast and maturation of the active site. Understanding these processes is important to improve HydA1-mediated H<sub>2</sub> production using Synthetic Biology tools and are described in the following sections. Most research studies to date have focused on HydA1 and less so on HydA2. Only where findings specifically involve HydA2, is it mentioned here.

*The transcription and translation of HydA1 occur under copper or O<sub>2</sub> deficiency*

As introduced earlier, *C. reinhardtii* has two hydrogenases, HydA1 and HydA2. Both belong to the [FeFe] A1 hydrogenase subclass and are localized in the chloroplast. HydA1 and HydA2 are encoded in the nucleus by *HydA1* and *HydA2*, respectively, and are translated by cytosolic ribosomes (Happe and Naber, 1993). HydA2 shares 68% protein sequence identity to HydA1 (Forestier *et al.*, 2003). Transcript levels of *C. reinhardtii* *HydA1*, *HydEF* and *HydG* are increased during anaerobiosis or copper deficiency and are regulated by the transcription factor copper response regulator I (CRR1) (Castruita *et al.*, 2011), in concert with potentially other unidentified

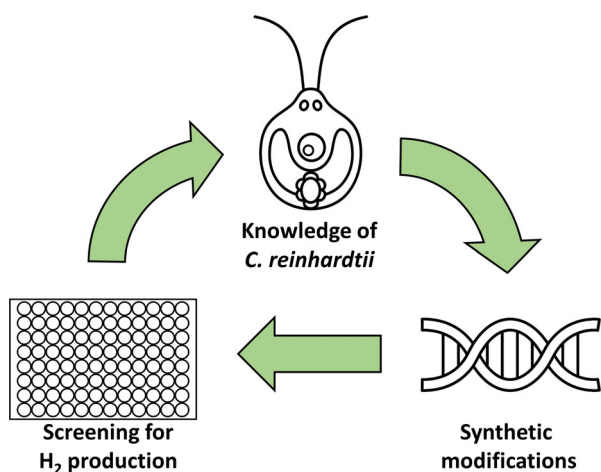


**Fig. 1.** Synthetic Biology Design Build Test Learn cycle for Improving H<sub>2</sub> production by *C. reinhardtii*. Knowledge of the biological systems involved in H<sub>2</sub> production by *C. reinhardtii* steers the design of synthetic modifications to H<sub>2</sub> production pathways. Synthetic constructs are built and screened for H<sub>2</sub> production, generating knowledge that can be used in future rounds of synthetic modification.

transcription factors (Pape *et al.*, 2012). HydA1 transcripts have also been shown to increase by 20% when inducing anaerobiosis by culturing *C. reinhardtii* cells in S depleted media (Gonzalez-Ballester *et al.*, 2010). Generally, it was found that transcript levels of *HydA1* reach a maximum 1.5–2 h after inducing anaerobiosis (Posewitz *et al.*, 2004b; Mus *et al.*, 2005), while functional HydA1 in chloroplasts was observed between 1 and 2 h post-anaerobiosis (Happe *et al.*, 1994).

Phototropic and autotrophic growth conditions affect the transcription of *HydA1* and *HydA2*. When culturing *C. reinhardtii* autotrophically, upon inducing anaerobiosis, the transcripts of *HydA1* and *HydA2* reached the maximum levels, threefold slower compared with cultures grown heterotrophically (i.e. in presence of acetate) (Forestier *et al.*, 2003). *HydA1/HydA2* transcripts also degrade more rapidly in presence of O<sub>2</sub> when *C. reinhardtii* is grown autotrophically, that is without acetate supplementation (Forestier *et al.*, 2003). These findings suggest that *HydA1/HydA2* transcription is initiated more rapidly and that the transcripts remain intact longer when *C. reinhardtii* is cultured heterotrophically in presence of an additional carbon source such as acetate. Acetate addition has been suggested to facilitate higher starch accumulation concomitant with faster respiratory O<sub>2</sub> consumption rates, which results in a more rapid onset of anoxia (Fouchard *et al.*, 2005). In support of this suggestion are the properties of a mutant of *C. reinhardtii* (*sta7-10* mutant) which is deficient in isoamylase activity, a starch hydrolysing enzyme. This mutant shows much lower *HydA1/HydA2* transcript levels compared with wild-type cells (Posewitz *et al.*, 2004b). The *HydA1/HydA2* transcripts' turnover rates in this *sta7-10* mutant are also enhanced, resulting in shorter H<sub>2</sub> photoproduction cycles (1.5 h) than observed for wild-type cells (> 10 h) under anoxic conditions (Posewitz *et al.*, 2004b). The wild-type phenotype could be restored in the *sta7-10* mutant strain through plasmid expression of the gene encoding the isoamylase enzyme. The results from this study support the hypothesis that supplementing the culture media with an additional carbon source is beneficial for extending the duration of H<sub>2</sub> production. The additional carbon source facilitates starch accumulation concomitant with the rapid occurrence of anoxia, and accumulation of *HydA1/HydA2* transcripts with slower degradation rates.

While HydA1/HydA2 enzymes are irreversibly damaged by O<sub>2</sub>, HydA1/HydA2 proteins are present in cells cultured aerobically under conditions where intracellular O<sub>2</sub> levels are quickly consumed due to high respiratory activities (Liran *et al.*, 2016; Kosourov *et al.*, 2018). However, HydA1/HydA2 protein levels typically increase with decreasing O<sub>2</sub> levels (Kosourov *et al.*, 2018).

### The import and maturation of HydA1 and HydA2

To be functionally active, HydA1 and HydA2 proteins first need to be imported into the chloroplast and matured. Following translation of *HydA1* and *HydA2* transcripts, the resulting pre-proteins are imported into the chloroplast stroma using the general import machinery that spans the chloroplast outer and inner membranes. This import machinery, known as the TOC-TIC import machinery (TOC for translocon at the outer envelope membrane of chloroplasts and TIC for translocon at the inner envelope membrane of chloroplasts), is a common feature in both plants and green algae and functions to import nuclear-encoded plastid proteins into the chloroplast (Bölter, 2018). An N-terminal chloroplast targeting sequence of 20–60 amino acids is required on the cytosolic protein to be imported by the TOC-TIC complex. The import targeting peptide becomes cleaved by a peptidyl processing protein protease after import into the chloroplast. Once imported, the HydA1/HydA2 proteins require maturation in the chloroplast to become active (Sawyer *et al.*, 2017). HydA1/HydA2 proteins are only functional when matured to their catalytically active form and under anoxic conditions (Kosourov *et al.*, 2018).

The maturation of HydA1 occurs through a stepwise biosynthesis and insertion of a H-cluster cofactor to form the active site of the enzyme (Britt *et al.*, 2020). The H-cluster is a characteristic feature of [FeFe] hydrogenases and consists of two Fe-S clusters, a 4Fe-4S cubane subcluster [4Fe-4S]<sub>H</sub> and a 2Fe subcluster [2Fe]<sub>H</sub> (Fig. 2) (Mulder *et al.*, 2010; Esselborn *et al.*, 2016). A cysteine S atom links [2Fe]<sub>H</sub> and [4Fe-4S]<sub>H</sub> together in the protein, constituting the full H-cluster active site (Britt *et al.*, 2020).

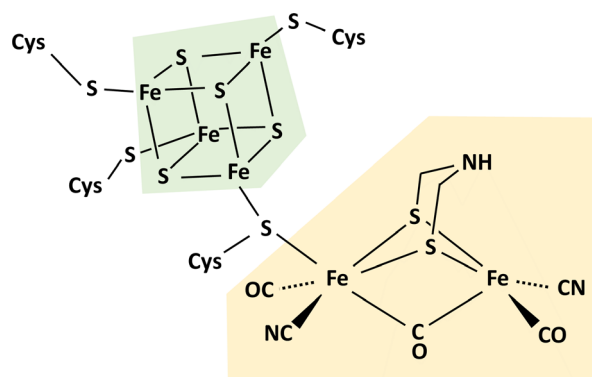


**Fig. 2.** Active site H-cluster of [FeFe] hydrogenases. The H-cluster constitutes two subclusters connected via a cysteine S: (i) [4Fe-4S]<sub>H</sub> (green), a classical 4Fe-4S cubane; and (ii) [2Fe]<sub>H</sub> (yellow), a unique di-iron Fe-S cluster coordinated with CO and CN ligands, and CO and azadithiolate bridges.

The [2Fe]<sub>H</sub> subcluster is a unique di-iron cluster found only in [FeFe] hydrogenases and is thought to be the active site of [FeFe] hydrogenases where H<sup>+</sup> or H<sub>2</sub> substrates bind (Mulder *et al.*, 2017; Pelmeshnikov *et al.*, 2017; Reijerse *et al.*, 2017; Land *et al.*, 2020). Both Fe atoms of the [2Fe]<sub>H</sub> subcluster have terminal CO and CN ligands, and the Fe atoms are further bridged by CO and azadithiolate ligands. The [2Fe]<sub>H</sub> subcluster is biosynthesized and inserted into HydA1 via the enzymes HydEF and HydG (Posewitz *et al.*, 2004a).

The [4Fe-4S]<sub>H</sub> subcluster balances the redox state of the enzyme and is required for hydrogenase activity (Rodríguez-Macia *et al.*, 2020). Four cysteine residues anchor the [4Fe-4S]<sub>H</sub> subcluster in [FeFe] hydrogenases (C115, C170, C362 and C366 in HydA1) (Kertess *et al.*, 2017). The housekeeping SUF Fe-S cluster assembly machinery synthesizes and inserts [4Fe-4S]<sub>H</sub> into the apo form of HydA1 followed by insertion of the [2Fe]<sub>H</sub> subcluster (Godman and Balk, 2008; Bai *et al.*, 2018). The order of insertion is supported by the requirement of [4Fe-4S]<sub>H</sub> to be present for [2Fe]<sub>H</sub> to produce a functional enzyme (Mulder *et al.*, 2009).

During O<sub>2</sub> inactivation of [FeFe] hydrogenases, the distal Fe of [2Fe]<sub>H</sub>, Fe<sub>d</sub>, is the first site to be 'attacked' and degraded by O<sub>2</sub>. In contrast, the [4Fe-4S]<sub>H</sub> cluster can remain stable in the presence of up to 17% O<sub>2</sub>. If the [4Fe-4S]<sub>H</sub> subcluster remains intact, the HydEF and HydG proteins can once again mature the [2Fe]<sub>H</sub> subcluster and the hydrogenase into its active state upon returning to hypoxic conditions (Swanson *et al.*, 2015).

#### Biosynthesis of [4Fe-4S]<sub>H</sub>

Green algae and plants have three different systems for assembly of 4Fe-4S clusters – (i) SUF, (ii) cytosolic Fe-S cluster assembly (CIA) and (iii) Fe-S cluster assembly (ISC) systems (Gomez-Casati *et al.*, 2021). Each of these 4Fe-4S cluster assembly systems operate in different parts of the cell. The SUF system in algae is localized in the chloroplast, the CIA system is in the cytosol, and the ISC system is in the mitochondria (Gomez-Casati *et al.*, 2021). Interestingly, the CIA system requires a functional ISC to work suggesting co-dependence between these two systems (Godman and Balk, 2008; Xu and Møller, 2011).

The synthesis and insertion of the H-cluster into HydA1 occurs after import into the chloroplast stroma, since folded or partially folded proteins cannot be transported across the chloroplast membranes by the TOC-TIC translocon (Paila *et al.*, 2015; Sawyer *et al.*, 2017). As such, the SUF system, and not CIA or ISC, is responsible for the assembly and insertion of [4Fe-4S]<sub>H</sub> into HydA1 and functions under O<sub>2</sub> and iron limitation conditions (Takahashi and Tokumoto, 2002; Pérard and Choudens, 2018).

The SUF-mediated 4Fe-4S cluster biosynthesis is poorly characterized in *C. reinhardtii*; however, it is well characterized in *E. coli* (Fig. 3) (Blahut *et al.*, 2020). *C. reinhardtii* produces 6 orthologues of the *E. coli* system: SufA, SufB, SufC, SufD, SufE and SufS (Godman and Balk, 2008). Sequence homology between the *C. reinhardtii* and *E. coli* SUF systems suggests they function similarly to produce 4Fe-4S clusters, although there is little direct experimental evidence to support this (Bai *et al.*, 2018). In *E. coli*, assembly of the Fe-S complex and transfer to the target protein is initiated by the cysteine desulfurase SufS and the S shuttling protein SufE forming the SufSE complex (Fig. 3) (Bai *et al.*, 2018; Pérard and Choudens, 2018; Blahut *et al.*, 2020). This SufSE complex then extracts S from cysteine and transfers it to a SufBC<sub>2</sub>D scaffold complex where the 4Fe-4S cluster is assembled (Fig. 3) (Bai *et al.*, 2018; Pérard and Choudens, 2018; Blahut *et al.*, 2020). Formation of the SufSE complex increases the cysteine desulfurase activity of SufS by 10- to 50-fold compared with free SufS. This increased activity has also been shown to be dependent on the sulfurization state of SufSE (Dai and Outten, 2012; Selbach *et al.*, 2013). Furthermore, SufBC<sub>2</sub>D in the presence of SufSE further increases the desulfurase activity of SufS 20- to 30-fold (Outten *et al.*, 2003; Dai and Outten, 2012). Evidence suggests that S from SufSE, electrons from FADH<sub>2</sub> and Fe from an unknown source are used to build the 4Fe-4S cluster at the SufB-SufD interface of SufBC<sub>2</sub>D (Pérard and Choudens, 2018; Blahut *et al.*, 2020). The synthesized 4Fe-4S cluster is then transferred to the carrier protein SufA which finally shuttles the assembled cluster to the target protein (Fig. 3) (Blahut *et al.*, 2020).

#### Biosynthesis of [2Fe]<sub>H</sub>

In *C. reinhardtii*, HydA1 containing a [4Fe-4S]<sub>H</sub> cluster acts as the site to which the [2Fe]<sub>H</sub> subcluster can bind to form the full H-cluster (Fig. 2). The formation and assembly of this [2Fe]<sub>H</sub> subcluster in [FeFe] hydrogenases require the activity from three maturase enzymes: the two radical S-adenosyl-L-methionine (rSAM) enzymes HydE and HydG, and a guanosine triphosphatase (GTPase) enzyme, HydF. The details of the different stages of the biosynthesis of the [FeFe] hydrogenase 2Fe subcluster by these three enzymes, HydE, HydF and HydG, have been described in a recent review and are summarized in Fig. 4 (Britt *et al.*, 2020).

The first step in the biosynthesis of the [2Fe]<sub>H</sub> subcluster is carried out by HydG. HydG is a free radical SAM enzyme that has two different Fe-S clusters sitting at each end of a conserved triosephosphate isomerase (TIM) barrel channel. These two Fe-S clusters carry out separate reactions to produce an Fe (II) intermediate

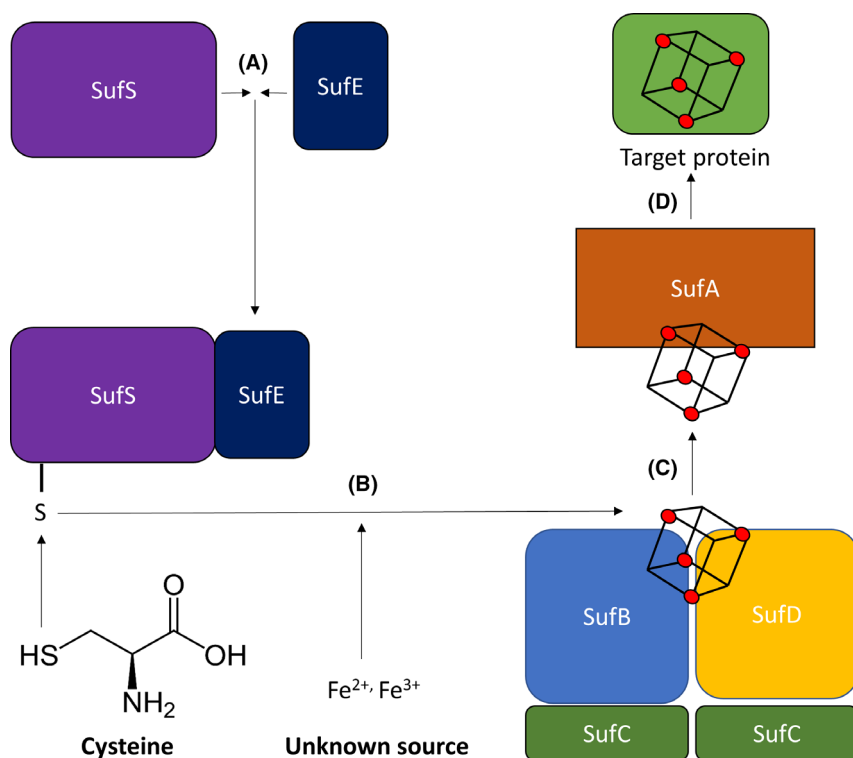


**Fig. 3.** Schematic Illustration of the SUF-mediated biosynthesis of [4Fe-4S] clusters in *E. coli*.

A. SufS binds SufE to form the SufSE complex, increasing the desulfurase activity of SufS up to 50-fold.

B. Sulfur is acquired from L-cysteine by the SufSE complex. The SufSE complex then binds with the scaffold complex SufBC<sub>2</sub>D, further increasing desulfurase activity by another 20- to 30-fold. Sulfur acquired from cysteine and iron from an unknown source is used to build the [4Fe-4S] cluster at the interface of SufB and SufD.

C. The complete [4Fe-4S] cluster (shown as a cubane molecule) is transferred to SufA.

D. SufA transports [4Fe-4S] to the target protein.

species. Specifically, the Fe-S cluster at the N-terminus of the TIM barrel channel is a [4Fe-4S] cluster and cleaves tyrosine to produce both the CO (Shepard *et al.*, 2010) and CN ligands (Driesener *et al.*, 2010). The Fe-S cluster at the C-terminal of the TIM barrel channel is a unique [5Fe-5S] cluster, having a classical [4Fe-4S] cubane structure linked to an auxiliary Fe via a bridging sulphide. Evidence points towards the auxiliary Fe of [5Fe-5S] acting as a receiver for coordination of the CO and CN ligands derived from the cleaved tyrosine (Dinis *et al.*, 2015). A second CO ligand, from a subsequent tyrosine cleavage, forms another bond with the auxiliary Fe, while the second CN coordinates with the cubane to form a [4Fe-4S-CN] complex, resulting in release of the Fe(II) intermediate species as shown in Fig. 4A (Suess *et al.*, 2015). This Fe(II) intermediate species made by HydG then binds with 5' deoxyadenosine of HydE, reducing the Fe(II) centre to Fe(I) as shown Fig. 4B (centre of figure) (Tao *et al.*, 2020). The Fe(I) intermediate species undergoes further reactions to eventually yield the [2Fe]<sub>H</sub> precursor, conceivably through pairwise condensation of the Fe(I) intermediate (Tao *et al.*, 2020). It is currently unclear whether the Fe(I) intermediate

condenses into the [2Fe]<sub>H</sub> precursor within HydE, as shown Fig. 4B (top of figure), or if the intermediate is transferred to HydF prior to the formation of this precursor (Britt *et al.*, 2020). Whether the formation of the CO and azadithiolate bridges are mediated by HydE or HydF remains unresolved. The addition of two serine molecules to form the azadithiolate bridge, Fig 3C (top), occurs by an unknown mechanism (Rao *et al.*, 2020). It has been suggested that one of the terminal CO ligands of the 2Fe precursor is reconfigured into the CO bridge. Whether or not HydF is involved in these final stages of [2Fe]<sub>H</sub> cluster biosynthesis is unclear. Evidence points towards HydF being involved with transfer of the complete [2Fe]<sub>H</sub> to [4Fe4S]<sub>H</sub> of HydA1 in the final stages of assembly of the H-cluster and hydrogenase maturation (Berggren *et al.*, 2013; Albertini *et al.*, 2015).

#### Hydrogen production pathways in *C. reinhardtii*

There are three pathways through which HydA1 produces H<sub>2</sub> in *C. reinhardtii*. These are photosystem (PS) II-dependent H<sub>2</sub> photoproduction, PS II-independent H<sub>2</sub> photoproduction and H<sub>2</sub> production during dark

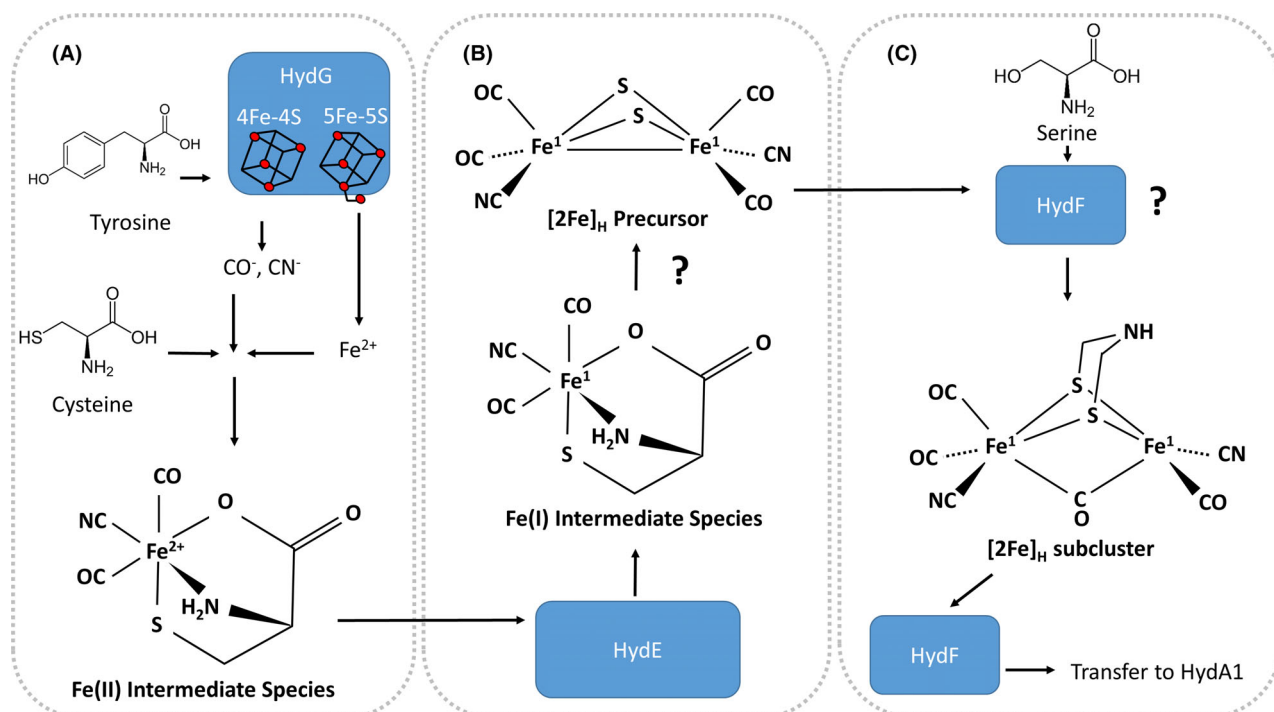


**Fig. 4.** Biosynthesis of the [2Fe]<sub>H</sub> subcluster.

A. HydG catalyses two reactions to form the Fe(II) intermediate species. Two tyrosine molecules are cleaved by [4Fe-4S] into CO and CN ligands. The auxiliary Fe of [5Fe-5S] is chelated by cysteine and coordinated by the CO and CN ligands to complete the intermediate.

B. The Fe(II) centre of the intermediate is reduced to Fe(I) by HydE. Subsequent reactions form the [2Fe]<sub>H</sub> precursor through an unknown mechanism; however, it has been suggested that the transformation occurs through pairwise condensation of the Fe(I) intermediate.

C. The [2Fe]<sub>H</sub> precursor is transformed into the final [2Fe]<sub>H</sub> subcluster by forming the azadithiolate and CO bridges. The mechanisms by which the bridges form are unclear; however, two serine molecules are involved in formation of the azadithiolate bridge with HydF possibly playing a role, and it has been suggested a terminal CO ligand on the [2Fe]<sub>H</sub> precursor is reconfigured into the CO bridge. The complete [2Fe]<sub>H</sub> subcluster is transferred to HydA1 by HydF.

anaerobic fermentation (Fig. 5). In each of these three pathways, electrons are donated to HydA1 through a reduced ferredoxin (Fd) species. There are eight Fd isoforms that have been shown or predicted to be expressed by the *C. reinhardtii* chloroplast (PetF, FDX2-3 and FDX5-9) (Sawyer and Winkler, 2017). The particular isoform that donates electrons to HydA1 is still up for debate, although PetF is hypothesized to fill this role. However, a recent transcriptome study has implicated FDX9 as the prime electron carrier as it is the only chloroplastic Fd isoform with an expression pattern that matches the expression of HydA1 and HydA2 over a 24-hr period during natural light/dark cycles (Strenkert *et al.*, 2019). For clarity, we will refer to the electron donor in the H<sub>2</sub> production pathway herein to be PetF as it is currently accepted as the isoform that donates electrons to HydA1.

Illuminating *C. reinhardtii* cells can activate either PS II-dependent or PS II-independent H<sub>2</sub> production (Chochois *et al.*, 2009). Hydrogen production by the PS II-dependent pathway occurs post-illumination when PS II is functioning normally. However, H<sub>2</sub> production via this pathway is a short-lived process, lasting only 6 min

(Ben-Zvi *et al.*, 2019). This time frame of H<sub>2</sub> production is rather impractical for commercial applications. The second pathway, the PS II-independent pathway, can be activated upon illumination by partly inhibiting PS II through nutrient deprivation, addition of the PS II specific inhibitor (DCMU), or genetically through modifying PS II gene expression. PS II-independent H<sub>2</sub> photoproduction has been shown to significantly prolong H<sub>2</sub> production for up to 200 h. However, inducing the PS II-independent route for H<sub>2</sub> production through nutrient deprivation limits cell growth (Chochois *et al.*, 2009). The third H<sub>2</sub> production pathway, which is activated through dark anaerobic fermentation, can be sustained for over 6 hours (Kanygin *et al.*, 2020). These three pathways are described in more detail in the following sections.

#### PS II-dependent photoproduction of hydrogen

During PS II-dependent photoproduction of H<sub>2</sub>, PS II absorbs photons via the light-harvesting complex (LHC) II antenna and splits water into protons, electrons and O<sub>2</sub> (Fig. 5, orange arrows). In general, the electrons are shuffled in a *linear* electron flow (LEF) across the

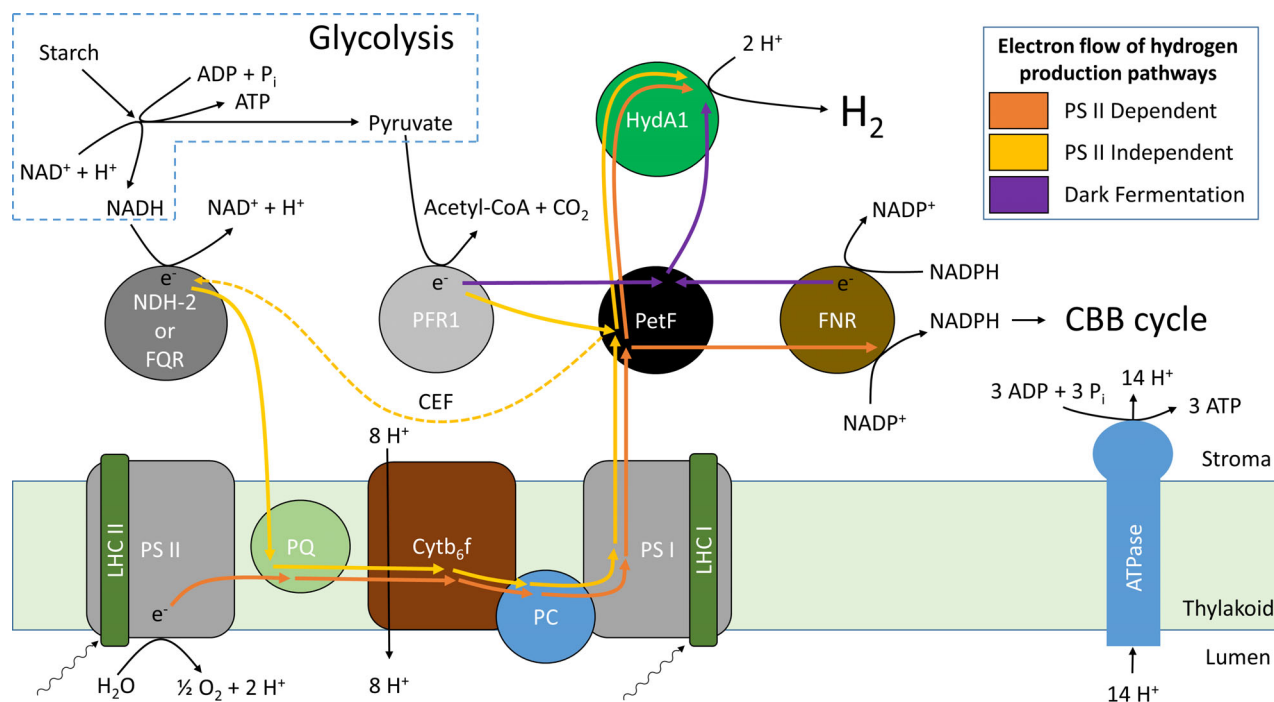


**Fig. 5.** H<sub>2</sub> production pathways in *C. reinhardtii*. Schematic illustration showing the photosystem (PS) II-dependent pathway (orange arrows), the PS II-independent pathway (yellow arrows) and the dark fermentation pathway (purple arrows). In all H<sub>2</sub> production pathways, reduced ferredoxin (PetF) supplies electrons to HydA1, which in turn catalyses the reduction in protons into H<sub>2</sub>. The photosynthetic electron transport chain (PETC) occurs as linear electron flow (LEF) (orange and yellow arrows) or circular electron flow (CEF) (yellow arrows, dashed). LHC, light-harvesting complex; Cytb<sub>6</sub>/f, cytochrome b<sub>6</sub>/f complex; PC, plastocyanin; FNR, ferredoxin reductase; FQR, ferredoxin-plastoquinone reductase; NDH-2, NAD(P)H-PQ oxidoreductase; PFR1, Pyruvate:Ferredoxin Oxidoreductase. Further details and references are described in the main text.

photosynthetic electron transport chain (PETC) via three pigment-proteins PS II, the b<sub>6</sub>/f cytochrome complex (Cytb<sub>6</sub>/f) and PS I. Electron transport between these three pigment-proteins is mediated by two electron carriers plastoquinone (PQ) and plastocyanin (PC). Both these proteins can freely diffuse through the lipid layers. Electrons leaving PS I are used to reduce PetF which then distributes the electrons to either NAD(P)H ferredoxin reductase (FNR) (the *primary* electron acceptor) or HydA1 (the *secondary* electron acceptor) (Hemschemeier and Happe, 2011; Sawyer and Winkler, 2017). FNR catalyses the reduction in NADP<sup>+</sup> into NADPH for use in the CBB carbon fixation cycle (Shin, 2004).

Hydrogen production via the PS II-dependent pathway has been shown to occur upon illuminating anoxic *C. reinhardtii* cells after they have been placed in the dark for a minimum of 30 min (Happe *et al.*, 1994). Hydrogen production typically begins at the onset of illumination and rates of H<sub>2</sub> evolution increase for ~2 min before steadily declining and ceasing at ~6-min post-illumination (Ben-Zvi *et al.*, 2019). These changes in rates of H<sub>2</sub> production resemble changes from LEF to *cyclic* electron flow (CEF) with CEF activity reaching a maximum at ~2 min post-illumination, and the activation

of the CBB cycle at ~2–4 min (Godaux *et al.*, 2015). When CEF occurs, electrons are cycling through PS I by channelling electrons from PetF back towards the PQ pool instead to FNR or HydA1 (Fig. 5, yellow, dashed arrow). These findings suggest PS II-dependent H<sub>2</sub> production is driven by PS I-CEF until the CBB cycle becomes active and the electron flux is entirely directed towards carbon assimilation.

By producing H<sub>2</sub>, HydA1 also removes protons from the stroma and thereby establishes a proton gradient for ATP synthesis by ATPase which is required for carbon assimilation (Fig. 5). Removing protons also results in the stroma becoming alkalized (pH 6.5 increases to pH 8.5), which is necessary for RuBisCO activity, the key enzyme of the CBB cycle. A pH change closely resembling the stromal pH change before and after illumination (pH 7 to pH 9) enhanced the HydA1-PetF rate constant for binding threefold *in silico* (Diakonova *et al.*, 2016).

One of the major factors contributing to the cessation of H<sub>2</sub> production 6-min post-illumination in the PS II-dependent pathway has been hypothesized to be the inactivation of HydA1 by O<sub>2</sub> (Ghirardi, 2015). However, recent evidence supports an alternative hypothesis where HydA1 activity ceases due to electron competition with FNR. For example, it was observed that electron



flow is channelled exclusively through FNR for carbon fixation *before* the irreversible inactivation of HydA1 by O<sub>2</sub> occurs (Milrad *et al.*, 2018; Ben-Zvi *et al.*, 2019). This alternative hypothesis is further supported by the observation that HydA1 can remain active in aerobically grown cultures as there are high rates of local respiratory O<sub>2</sub> consumption, creating microoxic niches at the stromal interface of the thylakoid membrane where HydA1 is typically located (Liran *et al.*, 2016). In these aerobic cultures, HydA1 was shown to be a minor sink for electrons leaving the PETC, particularly for reductants produced upon the transition from low to high light.

As intermittent H<sub>2</sub> production is problematic for scaled production, there has been ongoing efforts to prolong H<sub>2</sub> production via the PS II-dependent route. By exposing cultures to a cycle of very short (1 s) pulses of light followed by dark intervals (9 s), cultures can maintain low O<sub>2</sub> levels and H<sub>2</sub> production can be prolonged for up to three days (Kosourov *et al.*, 2018). Under such controlled light and dark cycling conditions, the maximum achieved reported rate of H<sub>2</sub> production was 25 μmol H<sub>2</sub> mg<sup>-1</sup> Chl h<sup>-1</sup>. However, given that chlorophyll concentration varies with cell density and growth conditions, these units of H<sub>2</sub> production are not particularly useful for comparing with other biological H<sub>2</sub> production rates in the literature which are typically presented as mmol H<sub>2</sub> l<sup>-1</sup> h<sup>-1</sup> (where l represents the cell culture volume). In this review, we have therefore recalculated and presented all H<sub>2</sub> production units as H<sub>2</sub> lL<sup>-1</sup> h<sup>-1</sup> using reported cell densities (where available) or using a medium cell density of at 1 × 10<sup>7</sup> cells per ml, and the reported chlorophyll amounts per cell of 2.4–3.5 × 10<sup>-15</sup> mol (Polle *et al.*, 2000). Thus, 25 μmol H<sub>2</sub> mg<sup>-1</sup> Chl h<sup>-1</sup> as reported above is equivalent to 0.37–0.54 mmol H<sub>2</sub> l<sup>-1</sup> h<sup>-1</sup>.

#### PS II-independent photoproduction of hydrogen

Hydrogen can also be produced via a PS II-independent pathway through partial inhibition of PS II (Fig. 5, yellow arrows). In this pathway, reduction in PQ occurs from electrons derived through oxidation of starch reserves and residual PS II activity. The non-photochemical reduction in the PQ pool by NAD(P)H is suggested to be mediated either through ferredoxin:plastoquinone oxidoreductase (FQR) or a type-II NADH dehydrogenase NAD(P)H-PQ oxidoreductase (NDH-2) (Courmac *et al.*, 2002; Mus *et al.*, 2005; Takabayashi *et al.*, 2005; Antal *et al.*, 2009). As per the PS II-dependent pathway, the reduced PQ pool then supplies electrons directly through Cytb<sub>6</sub>f to PS I. PS I then reduces PetF, which can feed electrons back to the PQ pool via CEF through FQR (Fig. 5, yellow, dashed arrows), or directly to HydA1 to generate H<sub>2</sub> (Fig. 5, yellow arrows) (Antal *et al.*, 2009). Competition for electrons from PetF between HydA1 and

CEF was shown to slow H<sub>2</sub> production more than two-fold (Antal *et al.*, 2009).

PS II-independent H<sub>2</sub> photoproduction in *C. reinhardtii* can be achieved by starving cells of S (Melis *et al.*, 2000) or phosphorus (P) (Batyrova *et al.*, 2012). It can also be achieved via magnesium (Mg) depletion, a key ion of chlorophyll, which is a main component of the two light-harvesting complexes LHC II and LHC I (Volgusheva *et al.*, 2015). All these nutrient depletion treatments result in impaired PS II assembly or repair and thus reduced PS II activity. The implications of a reduction in the PS II activity are both decreased O<sub>2</sub> evolution rates and carbon assimilation, which in turn leads to respiration and increased cellular stress levels.

There are four distinct cellular stages for cells that are nutrient-deprived and continuously illuminated. These are (i) O<sub>2</sub> increase and starch accumulation; (ii) decrease in O<sub>2</sub> levels; (iii) onset of anaerobiosis accompanied by starch degradation; and (iv) H<sub>2</sub> production (Nagy *et al.*, 2018). While starch accumulation during stage 1 and subsequent starch catabolism during stage 3 both contribute to H<sub>2</sub> production via the PS II-independent pathway, more than 92% of the electrons for H<sub>2</sub> production under nutrient-deprived conditions derive from light-driven water splitting as a result of residual PS II activity (Kosourov *et al.*, 2020).

Under nutrient limitation, H<sub>2</sub> production periods have been observed to last for up to 96 h for S-deprived cells (Nagy *et al.*, 2018), 150 h for P-deprived cells (Batyrova *et al.*, 2012) and 200 h for Mg-deprived cells (Volgusheva *et al.*, 2015). The maximum rates of H<sub>2</sub> production for these different conditions are 0.14–0.20 M h<sup>-1</sup> under S-deprivation (Kosourov *et al.*, 2003), ~0.05 M<sup>-1</sup> h<sup>-1</sup> under P-deprivation (at ~5.7 × 10<sup>-6</sup> cells) (Batyrova *et al.*, 2012) and 0.25–0.37 M h<sup>-1</sup> under Mg-deprivation (Volgusheva *et al.*, 2015). While these rates are lower than the 0.37–0.54 mmol H<sub>2</sub> l<sup>-1</sup> h<sup>-1</sup> observed in the PS II-dependent pathway (Kosourov *et al.*, 2018), the extended period of H<sub>2</sub> production increasing from a matter of minutes to over a week is an attractive quality for industrial biohydrogen production.

#### Dark fermentation production of hydrogen

A final pathway for H<sub>2</sub> production in *C. reinhardtii* is via dark fermentation (Fig. 5, purple arrows). Production of H<sub>2</sub> by dark fermentation is suggested to originate from oxidation of starch or other carbon sources and reduction in PetF by pyruvate ferredoxin oxidoreductase (PFR1) (Noth *et al.*, 2013), or the accumulation of NADPH from other catabolic processes causing FNR to operate in reverse, reducing Fd (Petrova *et al.*, 2020). Hydrogen production via dark fermentation is limited by the accumulation of fermentation products, notably acetic

acid, that can impair H<sub>2</sub> production and cell growth, and compete with other fermentation pathways in the cell (Fakhimi *et al.*, 2020). The rate of H<sub>2</sub> production by *C. reinhardtii* HydA1 during dark fermentation was reported to be nearly 50 times lower (~ 0.009–0.013 mmol H<sub>2</sub> l<sup>-1</sup> h<sup>-1</sup>) (Kanygin *et al.*, 2020) compared with PS II-independent H<sub>2</sub> photoproduction in Mg-deprived *C. reinhardtii* (~ 0.25–0.37 mmol H<sub>2</sub> l<sup>-1</sup> h<sup>-1</sup>) (Volgusheva *et al.*, 2015). Furthermore, H<sub>2</sub> production dark fermentation can be sustained for over 6 h (Kanygin *et al.*, 2020), significantly longer than the 6-min H<sub>2</sub> production period of PS II-dependent photoproduction (Ben-Zvi *et al.*, 2019), although much shorter than the 200 h H<sub>2</sub> production period of PS II-independent photoproduction (Volgusheva *et al.*, 2015).

### Strategies to improve H<sub>2</sub> production in *C. reinhardtii* using Synthetic Biology

A promising strategy for producing H<sub>2</sub> at industrial scale is by extending the *C. reinhardtii* H<sub>2</sub> production period through induction of the PS II-independent pathway. As such, efforts to induce the PS II-independent pathway using simpler methods than nutrient deprivation or expensive chemical inhibitors have been attempted. In addition to increasing the length of the H<sub>2</sub> production period, the efficiency of H<sub>2</sub> production needs to be improved in order to achieve the successful scaled production of H<sub>2</sub> in *C. reinhardtii*. Light-to-H<sub>2</sub> conversion efficiencies for *C. reinhardtii* are reported to be below 2% which is approximately 10% of the theoretical maximum (Kanygin *et al.*, 2020). Major factors contributing to the low H<sub>2</sub> production efficiency in *C. reinhardtii* include synthesis and maturation of active HydA1, O<sub>2</sub> sensitivity of HydA1 as well as competition for electrons between HydA1, FNR and CEF. In this next section, we discuss these limitations and how Synthetic Biology has helped to overcome them.

#### Genetic Engineering to alter H<sub>2</sub> production pathways

Synthetic Biology has been used to improve PS II-independent H<sub>2</sub> photoproduction in *C. reinhardtii*. In a synthetic *C. reinhardtii* strain, *cyc6Nac2.49*, expression of PS II was made inducible by fusing the *Nac2* gene to the *cyc6* promoter, which is induced under anaerobic conditions or copper deficiency (Surzycki *et al.*, 2007). *Nac2* is key for PS II expression as it binds to and stabilizes *psbD* mRNA, which translates to the PS II D2 protein. Addition of copper to *cyc6Nac2.49* cultures was shown to reduce expression of *Nac2* and diminished PS II D2 protein levels 8 h post-addition. Undetectable levels of PS II D2 coincided with reduction in PS II activity and reduced O<sub>2</sub> evolution rates, and resulted in H<sub>2</sub>

production rates of up to 0.18–0.27 mmol H<sub>2</sub> l<sup>-1</sup> h<sup>-1</sup>. However, H<sub>2</sub> production was sustained for only a short period of time (1.5 h) as PS II protein levels eventually recovered due to the onset of anaerobiosis, which restores expression of PS II D2 protein. The duration of H<sub>2</sub> production achieved here is 64-fold shorter than the 96 h reported for S-deprived cultures (Nagy *et al.*, 2018). By fusing other genes to the *cyc6* promoter and controlling O<sub>2</sub> or copper levels in the media, this inducible chloroplast gene expression system might be applied for other gene targets *C. reinhardtii* (Surzycki *et al.*, 2007).

In a follow-up study, this same strain (*cy6Nac2.49*) was then tested for H<sub>2</sub> production during multiple dark-low-light cycles (Batyrova and Hallenbeck, 2017). The authors demonstrated that during illumination, the typical steep rise of O<sub>2</sub> in the culture was diminished due to O<sub>2</sub>-induced downregulation of the engineered *Nac2-PsbD* system and diminished PS II expression. This resulted in a 10-fold lower O<sub>2</sub> accumulation overall than in the parental WT strain. As a consequence, increased H<sub>2</sub> production rates were observed, particularly under low light (10 W m<sup>-2</sup>). Through cycling of dark–light conditions, H<sub>2</sub> production could be sustained for over 30 h. While the rates were 4.5 higher than for the parental WT strain under these conditions, the resulting rates of the mutant strain (0.038–0.056 mmol H<sub>2</sub> l<sup>-1</sup> h<sup>-1</sup>) (Batyrova and Hallenbeck, 2017) are much lower compared with wild-type *C. reinhardtii* grown in S-deprived media (0.14–0.20 M<sup>-1</sup> h<sup>-1</sup>) (Kosourov *et al.*, 2003) and Mg-deprived media (0.25–0.37 M<sup>-1</sup> h<sup>-1</sup>) (Volgusheva *et al.*, 2015). In addition, the mutant strain (*cy6Nac2.49*) showed poor cell growth during photoheterotrophic conditions as starch did not accumulate in this anaerobically inducible PS II strain. Nevertheless, because this is a powerful example of sustaining H<sub>2</sub> production through an O<sub>2</sub> and copper-mediated genetic circuit, this strain might be an interesting target for further strain engineering (Batyrova and Hallenbeck, 2017).

In addition to degrading or inhibiting the function of PS II, the PS II-independent pathway can also be further improved to sustain H<sub>2</sub> production for longer periods of time by other methods. Approaches that do not degrade PS II are beneficial as long-term loss of PS II function inhibits growth of cells. As mentioned previously, H<sub>2</sub> production via the PS II-independent pathway competes for electrons with PS I-mediated CEF (Cournac *et al.*, 2002; Antal *et al.*, 2009; Ghysels *et al.*, 2013). Therefore, an effective strategy to increase PS II-independent photoproduction is by targeting the disruption of CEF. For example, treating cells with inhibitors of ferredoxin-plastoquinone reductase (FQR), a key mediator of CEF, was shown to increase PS II-independent H<sub>2</sub> photoproduction in S-starved cells, twofold, compared with untreated cells (Antal *et al.*, 2009).

Alternatively, increased H<sub>2</sub> production rates were also achieved by disrupting CEF using Synthetic Biology techniques. For instance, a randomly generated mutant library of *C. reinhardtii* was first screened for mutants in which the LHC is locked in state 1 to favour LEF over CEF using fluorescence screening and spectroscopy (Kruse *et al.*, 2005). Shortlisted mutants in which CEF was disrupted were then screened for enhanced H<sub>2</sub> production. This study has resulted in identification of a new mutant strain *Stm6* with H<sub>2</sub> production rates 5–13 times higher than that of the wild-type strain over a range of conditions including light intensity and culturing time (Kruse *et al.*, 2005).

Disruption of the CEF pathway and improved H<sub>2</sub> production has also been achieved by generating a *C. reinhardtii* knockout (KO) mutant (*pgr1*) incapable of producing the Proton Gradient Regulation-Like 1 (PGRL1) (Tolte *et al.*, 2011). PGRL1 is required for CEF in *C. reinhardtii* and was suggested to act as alternative FQR, a key protein for CEF (Fig 4) (Hertle *et al.*, 2013), and to interact with the proton gradient regulation 5 (PGR5) (Tolte *et al.*, 2011). In this *pgr1* KO mutant, an approximately fourfold increase in the short-term photoproduction rate and yield of H<sub>2</sub> during high-light exposure, compared with the wild-type strain, was reported (Tolte *et al.*, 2011). A similar improvement in H<sub>2</sub> photoproduction by this mutant of nearly fourfold compared with the wild type was observed under S-deprivation over 6 days.

The duration and thus yield of H<sub>2</sub> production via the PS II-independent pathway are strongly controlled by the electrochemical gradient across the thylakoid membranes which restricts electron flow towards HydA1 (Cournac *et al.*, 2002). This has been shown by the addition of an oxidative phosphorylation uncoupler (carbonyl cyanide-4-(trifluoromethoxy)phenylhydrazone (FCCP) (Cournac *et al.*, 2002) or deletion of *pgr5* (Johnson *et al.*, 2014) and/or *pgr1* (Steinbeck *et al.*, 2015) which were observed to diminish the thylakoid proton gradient and uncoupling of ATP synthesis from the membrane proton transport system. For example, when the chemical inhibitor FCCP is used, H<sub>2</sub> production yields were shown to increase 10-fold in a PS II deficient *C. reinhardtii* mutant (Cournac *et al.*, 2002), and by 37% in S-starved *C. reinhardtii* (Antal *et al.*, 2009) due to prolonged H<sub>2</sub> production. Similarly, the *pgr5* and *pgr1* single mutant and a *pgr5/pgr1* double *C. reinhardtii* mutants were reported to generate one of the highest H<sub>2</sub> production yields (610–850 ml H<sub>2</sub>/L culture) (Steinbeck *et al.*, 2015). The sustained H<sub>2</sub> production in these mutants was suggested to be a result of greater residual PS II activity than in WT cells, while the oxygen-sensitive hydrogenase was protected from O<sub>2</sub> for extended periods through increased rates of respiration

(O<sub>2</sub> consuming) (Steinbeck *et al.*, 2015). Engineering cells to uncouple ATP synthesis from the membrane proton transport system therefore seems to be a promising strategy to mimic the effects of FCCP and increase H<sub>2</sub> production in *C. reinhardtii*.

Disruption of the CEF pathway to increase H<sub>2</sub> production has also been done by generating a PS I-HydA2 fusion protein in a *C. reinhardtii*  $\Delta$ *HydA1*,  $\Delta$ *HydA2* double knockout mutant strain (Kanygin *et al.*, 2020). The authors intended to direct electrons towards HydA2 and H<sub>2</sub> production by eliminating competition of electrons with FNR. This was done by genetically fusing HydA2 to the PS I Fe-S centre C (PsaC), the terminal electron acceptor subunit of PS I. As a result, HydA2 intercepts electrons directly from PS I for H<sub>2</sub> production, which lasted up to 5 days. This strategy was extremely successful in efficiently mediating the electron flow directly between PS I and HydA2, and as such, bypassing both the CEF and FNR pathways. It was also successful in decreasing the O<sub>2</sub> evolution rates from PS II below the respirational O<sub>2</sub> consumption rates. The PsaC-HydA2 chimera showed a sevenfold increase in the rate of H<sub>2</sub> production at high-light intensity (2000  $\mu$ mol photons m<sup>-2</sup> s<sup>-1</sup>) compared with the WT strain which saturated at 100  $\mu$ mol photons m<sup>-2</sup> s<sup>-1</sup>. Such high-light intensities are usually detrimental to H<sub>2</sub> photoproduction as the O<sub>2</sub> evolution rates by PS II also increase under these conditions (Batyrova and Hallenbeck, 2017). In addition to the disruption of CEF, the CBB cycle was significantly down-regulated. However, the ability of PetF to intercept electrons away from HydA2 remained. Overall, the efficiency of the conversion of light to H<sub>2</sub> was reported as 1.75%. This efficiency is only about 10% of the theoretical maximum (Kanygin *et al.*, 2020) and over twofold short of the 5% efficiency target at which algal H<sub>2</sub> production is stated to be economically viable (Kruse *et al.*, 2005). Further engineering the PetF binding site of HydA2 and O<sub>2</sub> sensitivity was suggested to be an important next step to further improve H<sub>2</sub> production.

#### *Optimizing the stable expression of a functional HydA1*

Controlling the synthesis and maturation of HydA1 to optimize its protein yields and stability in *C. reinhardtii* is another important target for improving H<sub>2</sub> production. A strategy to regulate the synthesis and maturation of HydA1 is to express HydA1 from the chloroplast genome under controllable conditions. The presence of homologous recombination in *C. reinhardtii* chloroplasts makes this strategy more feasible than genetic engineering of the nucleus, where non-homologous DNA end-joining dominates. Additionally, expression of HydA1 in the chloroplast overcomes the need for protein import and the regulatory elements involved.

Using the native chloroplast homologous recombination system, HydA1 was integrated into the chloroplast genome of *C. reinhardtii* (Reifschneider-Wegner *et al.*, 2014). Integration of the synthetic gene design into the chloroplast genome required extremely tight regulation of *HydA1* expression using a double repressor system induced by vitamin B12 and thiamine pyrophosphate (TPP) due to a strong selective pressure against the synthetic *HydA1*. As a consequence, stable integration into the chloroplast genome was only achieved when culturing the cells in the dark making H<sub>2</sub> photoproduction unfeasible.

Nevertheless, engineered strains were able to produce HydA1 transcripts and apoprotein under both aerobic and anaerobic conditions and increased H<sub>2</sub> production yields during dark fermentation twofold when compared to its parent strain (Reifschneider-Wegner *et al.*, 2014). Therefore, this strain might be a good starting point for further strain engineering, to allow for inducible H<sub>2</sub> production through the more efficient PS II pathway and PS II-independent pathway.

#### *Heterologous and engineered hydrogenases with improved O<sub>2</sub> tolerance*

Native *C. reinhardtii* HydEF and HydG maturases in conjunction with native [4Fe-4S] cluster machinery was demonstrated to be capable of maturing heterologous [FeFe] hydrogenases such as Cpl from *C. pasteurianum* (Sawyer *et al.*, 2017). The capacity of HydEF and HydG to mature heterologous [FeFe] hydrogenases in this study was suggested to be due to the homology of the H-cluster between [FeFe] hydrogenases.

As mentioned earlier, a major limitation for photoproduction of H<sub>2</sub> in *C. reinhardtii* is the O<sub>2</sub> sensitivity of the [FeFe] hydrogenases (Ghirardi, 2015). To improve the tolerance of *C. reinhardtii* to O<sub>2</sub>, expression of heterologous hydrogenases in *C. reinhardtii* has been explored to find more O<sub>2</sub> tolerant enzyme variants. For example, Cpl expressed heterologously from the *C. reinhardtii* chloroplast demonstrated higher O<sub>2</sub> tolerance than HydA1/HydA2 (Noone *et al.*, 2017). Additionally, H<sub>2</sub> production in *C. reinhardtii* using a double point mutated variant of Cpl (Cpl<sup>T356V/S357T</sup>) (Koo and Swartz, 2018) showed improved O<sub>2</sub> tolerance, retaining 85% of initial activity after exposure to O<sub>2</sub> compared to 65% for the wild type (Elman *et al.*, 2020).

More recently, another clostridial [FeFe] hydrogenase, CbA5H from *C. beijerinckii*, was shown to be O<sub>2</sub> tolerant (Winkler *et al.*, 2021). CbA5h is the only [FeFe] hydrogenase shown to protect the H-cluster from destruction by long-term O<sub>2</sub> exposure. When CbA5h is exposed to air, the H-cluster changes from an active state to an inactive O<sub>2</sub> protected state (H<sub>inact</sub>). The formation of H<sub>inact</sub> is

dependent on the conserved cysteine residue C367, which is thought to act as a safety cap for the H-cluster preventing O<sub>2</sub> attack. In the H<sub>inact</sub> state, residue C367 is in close proximity (3.1 Å) to the distal Fe atom, Fe<sub>d</sub>, of the 2Fe cluster, which is the site of degradation of the H-cluster by O<sub>2</sub> in other [FeFe] hydrogenases (Swanson *et al.*, 2015). The C367-Fe<sub>d</sub> distance is only slightly longer than the average distance for covalent Fe-S bonds (2.4 Å) and is small enough to stop small molecules including H<sub>2</sub> and O<sub>2</sub> from inserting between Fe<sub>d</sub> and C367. By comparison, the distance between Fe<sub>d</sub> and the corresponding cysteine residue (C299) of Cpl from *C. pasteurianum* is significantly longer (5.1 Å) accounting for the inability of Cpl to enter the H<sub>inact</sub> state. Residues L364, A561 and P386, which are in close proximity to the H-cluster in CbA5H, also contribute to increased O<sub>2</sub> resistance of CbA5h. The mechanisms of O<sub>2</sub> tolerance in CbA5H are similar to [NiFe] hydrogenases, where two conserved cysteine motifs in close proximity to the proximal Fe-S cluster confer O<sub>2</sub> tolerance to the hydrogenase (Lukey *et al.*, 2011).

#### *Diverting electron flow to HydA1*

During illumination and photosynthesis by PS II, FNR is the primary electron acceptor of the PETC transferring electrons from reduced PetF to NADP<sup>+</sup> generating NADPH for carbon fixation (Shin, 2004). While photosynthesis is concomitant with O<sub>2</sub> evolution, which itself inhibits HydA1 activity, it was suggested that HydA1 is outcompeted for electrons from PetF by FNR prior to the inactivation of HydA1 by O<sub>2</sub> (Milrad *et al.*, 2018; Ben-Zvi *et al.*, 2019). As such, competition for electrons between HydA1 and FNR is hypothesized to be a major limitation during PS II-dependent H<sub>2</sub> photoproduction. FNR protein levels are approximately 70-fold higher than that of HydA1 in *C. reinhardtii* (Nikolova *et al.*, 2018) and the affinity of FNR to PetF is 4- to 13-fold higher than that of HydA1 (K<sub>m</sub> (FNR) = 0.8–2.6 mM, K<sub>m</sub> (HydA1) = 3.4–35 mM) (Kanygin *et al.*, 2020). Thus, a strategy for improving H<sub>2</sub> photoproduction by *C. reinhardtii* has been to engineer proteins to increase the interaction of PetF with HydA1 rather than FNR (Sawyer and Winkler, 2017). A PetF-HydA1 fusion protein was shown to successfully divert over 60% of the photosynthetic electron pool towards H<sub>2</sub> production *in vitro* compared with less than 10% observed for HydA1 (Yacoby *et al.*, 2011). This fusion protein also improved H<sub>2</sub> production 4.5-fold *in vivo* compared with the wild type when expressed in *C. reinhardtii* (Eilenberg *et al.*, 2016). The increase in H<sub>2</sub> production was attributed to a tethering of PetF-HydA1 to PS I allowing for effective interception of photosynthetic electrons. The fusion protein also showed improved O<sub>2</sub> resistance *in vitro* and *in vivo*, retaining

25% activity after 10-min exposure to O<sub>2</sub> (1.7 μmol) compared to 7.5% activity for wild-type HydA1 (Eilenberg *et al.*, 2016). The PetF moiety of the HydA1-PetF fusion was hypothesized to either reduce O<sub>2</sub> to O<sub>2</sub><sup>-</sup>, which cannot penetrate the active site of HydA1 due to its charge, or partially block O<sub>2</sub> to access the pathway leading to the active site of HydA1 (Eilenberg *et al.*, 2016).

In another study, a double mutant *C. reinhardtii* PetF construct (D19A/D58A) produced by site-directed mutagenesis showed a fourfold improved H<sub>2</sub> production *in vivo* (Rumpel *et al.*, 2014). The PetF double mutant construct showed a reduced affinity for FNR, and so photosynthetic electrons were more likely to be directed towards HydA1 and H<sub>2</sub> production. More recently, site-directed mutagenesis of FNR and Fd from *Synechocystis* PCC 6803 was undertaken to assess the protein to protein interaction with recombinant HydA1 from *C. reinhardtii* (Wiegand *et al.*, 2018). Single amino acid exchange of aspartate to alanine near the C terminus (Fd-D22A) and the N-terminus (Fd-D61A) of Fd increased Fd-HydA1 interaction and H<sub>2</sub> photoproduction by 15 and 23% respectively (Wiegand *et al.*, 2018). Exchange of a lysine residue to aspartate near the N-terminus of the cyanobacterial FNR (FNR-K78-D), together with the Fd-D61A mutant, significantly decreased Fd/FNR interaction and conversely increased Fd/HydA1 interaction and H<sub>2</sub> photoproduction *in vitro* by 18-fold (Wiegand *et al.*, 2018). Modifications to HydA1 to improve binding affinity for PetF have not yet been explored but could further improve H<sub>2</sub> production. This is a challenging task, suggested to likely require directed evolution rather than rational site-directed mutagenesis (Sawyer and Winkler, 2017).

A HydA1 and superoxide dismutase (SOD) fusion protein, originally designed to increase the O<sub>2</sub> tolerance of HydA1, greatly enhanced H<sub>2</sub> production (Ben-Zvi and Yacoby, 2016). While the HydA1-SOD fusion protein did not protect HydA1 from O<sub>2</sub>, the fusion protein showed H<sub>2</sub> production up to 10–15 mmol H<sub>2</sub> l<sup>-1</sup> h<sup>-1</sup> in *C. reinhardtii*, the highest photosynthetic rate of H<sub>2</sub> production reported to date. The HydA1-SOD fusion protein was also shown to produce H<sub>2</sub> continuously for up to 14 days. This was hypothesized to be due to the ability of the HydA1-SOD fusion protein to compete with the CBB cycle for photosynthetic electrons, and reduced O<sub>2</sub> evolution (Ben-Zvi *et al.*, 2019). This extended H<sub>2</sub> production period was also achieved with non-limiting media rather than using nutrient-deprived media that is typically used to activate PS II-independent H<sub>2</sub> photoproduction. The majority of electrons for H<sub>2</sub> production using HydA1-SOD were shown to be supplied by PS II LEF, with starch catabolism playing a secondary role. The competition with CBB does have some drawbacks, as *C. reinhardtii* HydA1-SOD mutants had slower growth rates,

likely due to the reduced flux through the CBB cycle and impaired photosynthetic activity. The molecular mechanism accounting for this improved H<sub>2</sub> production by HydA1-SOD is unclear, although two hypotheses were put forward. First was that HydA1-SOD may be bound to or in close proximity to PS I, hindering the access of FNR to reduced PetF. The alternate hypothesis was that HydA1-SOD outcompetes soluble FNR for electrons in the stroma (Ben-Zvi *et al.*, 2019).

### High-throughput screening tools of hydrogenase activity

Screening of large libraries of synthetic, engineered or native hydrogenases and other proteins involved in biological H<sub>2</sub> production for improved H<sub>2</sub> production in *C. reinhardtii* ideally requires accurate, efficient and reliable HTS platforms. These HTS platforms can be automated and integrated in automated strain engineering pipelines. While several instruments and methods are available to sensitively assay biological H<sub>2</sub> production, such as the Clark-type electrode (normally used for measuring dissolved O<sub>2</sub>) in reverse polarity configuration (Mišlov *et al.*, 2015) or gas chromatography (Weijun, 2015), these methods can be slow and cumbersome and are typically low-throughput. In order to process large sample numbers, HTS methods (Ghirardi, 2015) have been developed which include chemochromic films (Posewitz *et al.*, 2004b); biochemical assays using sulfonated Wilkinson's catalyst with a tetrazolium indicator (Schrader *et al.*, 2008); methyl-viologen assays in combination with cell-free synthesis using single-molecule PCR expression (SIMPLEX) (Stapleton and Swartz, 2010a); *in vitro* compartmentalization using C<sub>12</sub>-resorufin fluorescence (Stapleton and Swartz, 2010b); or a *Rhodobacter capsulatus* H<sub>2</sub> biosensor (Wecker and Ghirardi, 2014). Another high-throughput method that can be considered is the use of chemically synthesized [2Fe]<sub>H</sub> cluster mimics which can be used to artificially mature the [FeFe] hydrogenases (Land *et al.*, 2019). These HTS assays and their applications for characterizing hydrogenases and measuring H<sub>2</sub> production are briefly described in the following sections. With the exception of chemochromic films and the *Rhodobacter* biosensor, the HTS assays for measuring H<sub>2</sub> typically rely on redox reactions of the hydrogenase with a non-natural substrate, and hence the measured rates *in vitro* might not always reflect H<sub>2</sub> production *in vivo*.

#### *Pd/WO<sub>3</sub>* chemochromic films

Chemochromic films are composed of Pd/WO<sub>3</sub> layers that turn blue when reduced by H<sub>2</sub>. These films are very sensitive to H<sub>2</sub> and can detect amounts of H<sub>2</sub> as low as

4 nmol (Siebert *et al.*, 2001). Pd/WO<sub>3</sub> chemochromic films have been used to measure H<sub>2</sub> production in a strain of *C. reinhardtii* containing a mutated and non-functional isoamylase gene, *STA7* (Posewitz *et al.*, 2004b). As *STA7* is involved in the accumulation of starch, the decrease in H<sub>2</sub> production detected by the films provided a clear link of starch degradation to H<sub>2</sub> production by dark fermentation (Posewitz *et al.*, 2004b). In another study, Pd/WO<sub>3</sub> chemochromic films were used in a high-throughput H<sub>2</sub> production assay device (H<sub>2</sub>PAD) to screen over 10,000 *C. pasteurianum* Cpl hydrogenase mutants and 400 *Oryza sativa* FNR mutants, identifying a hydrogenase with threefold higher H<sub>2</sub> turnover rate than wild-type Cpl, and an FNR mutant that increased NADPH-driven H<sub>2</sub> production by 60% (Koo *et al.*, 2017). The H<sub>2</sub>PAD device consisted of a 96-well plate at the bottom where biological H<sub>2</sub> production took place, a filter plate containing a desiccant (CaSO<sub>4</sub>) and at the top the Pd/WO<sub>3</sub> sensor plate.

#### Sulfonated Wilkinson's catalyst with tetrazolium indicator

Biological H<sub>2</sub> production is also effectively measured using a semi-quantitative colorimetric assay containing a water-soluble tetrazolium indicator (WST-3) and soluble Wilkinson's catalyst (Schrader *et al.*, 2008). This method was used to measure H<sub>2</sub> production by *Synechocystis* sp. PCC 6803 encapsulated in silica sol-gel (Dickson *et al.*, 2009). Wilkinson's catalyst is used to catalyse the hydrogenation of primary and secondary alkenes. In this assay, the Wilkinson's catalyst hydrogenates the tetrazole ring of WST-3, forming a formazan molecule which can be detected via a colour change at 433 nm. While not as sensitive as Pd/WO<sub>3</sub> chemochromic film based assays, the colorimetric assay using Wilkinson's catalyst has been shown to detect H<sub>2</sub> from whole-cell systems in microtitre plates for amounts of H<sub>2</sub> as low as 20 nmol (Schrader *et al.*, 2008).

#### SIMPLEX-based methyl-viologen HTS assay

Single-molecule PCR-linked expression (SIMPLEX) in conjunction with cell-free protein synthesis (CFPS), methyl-viologen reduction and gas chromatography (GC) has been used to screen the effects of hydrogenase mutations on H<sub>2</sub> production *in vitro*. After screening ~30,000 *hydA1* mutants with the SIMPLEX-based assay, a novel HydA1 mutant was identified which showed fourfold improved H<sub>2</sub> production compared with the wild type (Stapleton and Swartz, 2010a). SIMPLEX can amplify single molecules of DNA from a mutant library after serial dilution into microtitre plates. Subsequent expression of the mutant DNA using CFPS results in the plate wells containing on average just 2 mutant

proteins which can then be characterized using high-throughput assays. After amplification with SIMPLEX and expression with CFPS, H<sub>2</sub> consumption rates of hydrogenases are measured using methyl viologen as substrate. Methyl viologen can be an electron donor and acceptor for [FeFe] hydrogenases similar to PetF. Hydrogenases that oxidise H<sub>2</sub> in solution reduce methyl viologen which is indicated by a colour change from clear to blue, detectable at 578 nm. Following identification of high H<sub>2</sub> consumers, a shortlist of promising hydrogenases can then be analysed for their H<sub>2</sub> production rates using low-throughput techniques such as GC. A particular advantage of the SIMPLEX-based assay is the accelerated protein expression offered by CFPS compared with the typically slow-growing *C. reinhardtii*.

#### *In vitro* compartmentalization and fluorescence-activated cell sorting

A HTS for O<sub>2</sub> tolerance has been developed using a combination of *in vitro* compartmentalization (IVC), microbead display and fluorescence-activated cell sorting (FACS) (Stapleton and Swartz, 2010b). The throughput of IVC-FACS screening is significantly greater than 96-well plate assays and is able to sort > 1000 beads per second. This HTS tool is based on beads which bind to the DNA templates and are emulsified into droplets to create individual CFPS reactors. To demonstrate the suitability of this technique, a mock library of *C. pasteurianum* hydrogenase Cpl was successfully screened for O<sub>2</sub> tolerance. For this, streptavidin-coated beads are generated that each displayed a single biotinylated DNA template and biotinylated anti-hemagglutinin (HA) antibodies. The beads are then emulsified to form oil phase emulsion droplets to express hydrogenase proteins using emulsion CFPS (eCFPS). *E. coli* extracts containing the [FeFe] hydrogenase maturases HydE, HydF and HydG from *Shewanella oneidensis* are included in the emulsions to mature the hydrogenases. The hydrogenases contain three HA tags which once expressed bind to the anti-HA antibodies on the streptavidin-coated beads. After protein synthesis, the beads are removed from the emulsion droplets, washed and exposed to O<sub>2</sub>. New emulsion droplets containing the beads and the reporter molecule C<sub>12</sub>-resazurin are created after O<sub>2</sub> exposure. C<sub>12</sub>-resazurin forms a fluorescent molecule C<sub>12</sub>-resorufin when reduced by active hydrogenases in a H<sub>2</sub> consumption assay. Subsequently, the beads are again removed from the emulsion and FACS is used to detect and enrich fluorescent beads which contain hydrogenases that are tolerant to O<sub>2</sub> exposure. Since the beads still bind the respective DNA template, a direct genotype-phenotype link can be established to provide the sequence to the O<sub>2</sub> tolerant hydrogenase. While this

particular assay was tested to screen for O<sub>2</sub> tolerance of hydrogenases, it is useful for screening other important hydrogenase characteristics including thermostability and tolerance to other harsh conditions. The IVC-FACS assay was also confirmed to be compatible with HydA1 from *C. reinhardtii*, indicating that this screening platform may be used to screen [FeFe] hydrogenases from diverse organisms for a variety of characteristics (Stapleton and Swartz, 2010b).

#### *Rhodobacter biosensor*

A *Rhodobacter capsulatus* H<sub>2</sub> biosensor has been engineered to fluoresce upon exposure to H<sub>2</sub> (Wecker *et al.*, 2011). This organism has a H<sub>2</sub> sensory system composed of a H<sub>2</sub> sensor protein (HupUV), a histidine kinase (HupT), a transcription regulator (HupR) and an uptake hydrogenase (HupSL). The fluorescent reporter emGFP was inserted downstream of HupSL on a plasmid in *E. coli* S17-1 and transferred by conjugation into the recipient strain *R. capsulatus* JP91. After exposing the *R. capsulatus* biosensor to 0.1% H<sub>2</sub> for 4 h, the activation of emGFP by 1% O<sub>2</sub> exposure for 2 h was found to be sufficient to generate a fluorescent signal that was approximately eightfold higher than cells not exposed to H<sub>2</sub>. The lower limit of detection using the biosensor was 200 pM H<sub>2</sub> in solution. A 1:1 ratio of *C. reinhardtii* and the *R. capsulatus* biosensor was co-cultured in microtitre plates incubated under dark anaerobic conditions, followed by activation of emGFP by O<sub>2</sub> exposure. Fluorescent measurements of the co-culture correlated with H<sub>2</sub> concentrations in the headspace gas measured by GC.

The *R. capsulatus* biosensor has since been adapted for use on solid media to rapidly test for H<sub>2</sub> production by overlaying the biosensor, grown on agar, over single colonies of H<sub>2</sub> producing strains (Wecker and Ghirardi, 2014). The biosensor was recently used to assay the O<sub>2</sub> tolerance of *Clostridium pasteurianum* Cpl mutants expressed heterologously in *C. reinhardtii*, identifying the O<sub>2</sub> tolerant Cpl<sup>T356V/S357V</sup> mutant (Elman *et al.*, 2020). The advantage of this assay is that it measures actual H<sub>2</sub> production of the cells and not reduction in alternative, non-native substrates.

#### *Artificial maturation using [2Fe]<sub>H</sub> mimics*

Recently, a HTS assay for recombinant [FeFe] hydrogenases in *E. coli* was described that circumvents the expression of HydEF and HydG (Land *et al.*, 2019). When heterologously expressed in *E. coli*, [FeFe] hydrogenases lacking the [2Fe]<sub>H</sub> subcluster were artificially matured with a [2Fe]<sub>H</sub> subcluster mimic, [Fe<sub>2</sub>(adt)(CO)<sub>4</sub>(CN)<sub>2</sub>]<sup>2-</sup> ([2Fe]<sup>adt</sup>) to produce the functional enzyme (Berggren *et al.*, 2013; Esselborn *et al.*, 2013; Birrell

*et al.*, 2016; Caserta *et al.*, 2016; Chongdar *et al.*, 2018). In this way, artificial maturation with ([2Fe]<sup>adt</sup>) enables the screening of [FeFe] hydrogenases without co-expression of HydEF and HydG. This approach simplifies any HTS assay and allows for screening of mutants that may not be able to be matured by HydEF and HydG. After artificial maturation, the hydrogenases were assayed for H<sub>2</sub> production using reduced methyl viologen, complemented with protein film electrochemistry, whole-cell electron paramagnetic resonance (EPR) and Fourier transform infrared (FTIR) spectroscopy (Land *et al.*, 2019). Together, these techniques allow a more complete characterization of hydrogenases through quantification of expression levels and turnover frequency. This study was the first to employ protein film electrochemistry to characterize hydrogenases. The combined use of these techniques helped to characterize the hydrogenase Tam-HydA from *Thermoanaerobacter mathranii*, which showed a relatively low rate of H<sub>2</sub> production of 0.45 ± 0.18 μmol H<sub>2</sub> min<sup>-1</sup> l<sup>-1</sup> OD<sub>600</sub><sup>-1</sup>, being eightfold lower compared with *C. reinhardtii* HydA1 (3.6 ± 0.30 μmol H<sub>2</sub> min<sup>-1</sup> l<sup>-1</sup> OD<sub>600</sub><sup>-1</sup>), and which led to the discovery that this enzyme has predominantly a H<sub>2</sub> sensory function rather than a catalytic function. Further use of these combined techniques will be useful in future efforts to discover more efficient hydrogenases.

#### **Conclusion and future perspectives**

Many of the fundamental processes that drive H<sub>2</sub> production in *C. reinhardtii* have been described. Knowledge of these processes in conjunction with the genetic engineering tools of *C. reinhardtii* and target proteins have been used to improve H<sub>2</sub> production in *C. reinhardtii*. The major strategies explored were redirecting electron flow towards H<sub>2</sub> production, improving hydrogenase O<sub>2</sub> tolerance and using heterologous hydrogenases which may prove to be valuable for industrial biohydrogen production scales. Methods for assaying biological H<sub>2</sub> production are also now moving towards HTS which allows mutant libraries or more hydrogenase variants to be more rapidly screened, accelerating the synthetic biology 'design-build-test' cycle. Future efforts to improve H<sub>2</sub> production in *C. reinhardtii* should try to combine the proposed engineering targets mentioned above and select an appropriate HTS assay to efficiently screen the new constructs. In addition, new tools such as genetic circuits could be developed to couple H<sub>2</sub> production to growth or positive selection to support enrichment of mutants with superior H<sub>2</sub> producing traits. This use of selective pressure would allow for more randomized, evolutionary engineering approaches such as directed evolution and adaptive laboratory evolution which can rapidly increase the genetic diversity and broaden the

scale of the engineering. Altogether, knowledge of the fundamental processes underlying H<sub>2</sub> production in *C. reinhardtii*, discovery of O<sub>2</sub> tolerant hydrogenases, ever-evolving synthetic biology tools and development of HTS platforms has the potential to improve biological H<sub>2</sub> production to the point where it is economically viable to produce at an industrial scale.

### Acknowledgements

SK is supported by a Macquarie University RTP Scholarship. TJ and KP are supported by the Australian Renewable Energy Agency (ARENA) grant RW0003 awarded to RDW and LB.

### Conflict of interest

The authors declare no conflict of interest.

### References

- Albertini, M., Galazzo, L., Maso, L., Vallese, F., Berto, P., De Rosa, E., *et al.* (2015) Characterization of the [FeFe]-hydrogenase maturation protein HydF by EPR techniques: insights into the catalytic mechanism. *Top Catal* **58**: 708–718.
- Antal, T.K., Volgusheva, A.A., Kukarskih, G.P., Krendeleva, T.E., and Rubin, A.B. (2009) Relationships between H<sub>2</sub> photoproduction and different electron transport pathways in sulfur-deprived *Chlamydomonas reinhardtii*. *Int J Hydrog Energy* **34**: 9087–9094.
- Bai, Y., Chen, T., Happe, T., Lu, Y., and Sawyer, A. (2018) Iron-sulphur cluster biogenesis via the SUF pathway. *Metalomics* **10**: 1038–1052.
- Batyrova, K., and Hallenbeck, P.C. (2017) Hydrogen production by a *Chlamydomonas reinhardtii* strain with inducible expression of photosystem II. *Int J Mol Sci* **18**: 647.
- Batyrova, K.A., Tsygankov, A.A., and Kosourov, S.N. (2012) Sustained hydrogen photoproduction by phosphorus-deprived *Chlamydomonas reinhardtii* cultures. *Int J Hydrog Energy* **37**: 8834–8839.
- Ben-Zvi, O., Dafni, E., Feldman, Y., and Yacoby, I. (2019) Re-routing photosynthetic energy for continuous hydrogen production *in vivo*. *Biotechnol Biofuels* **12**(1): 266.
- Ben-Zvi, O., and Yacoby, I. (2016) The in-vitro enhancement of FeFe hydrogenase activity by superoxide dismutase. *Int J Hydrog Energy* **41**: 17274–17282.
- Berggren, G., Adamska, A., Lambert, C., Simmons, T.R., Esselborn, J., Atta, M., *et al.* (2013) Biomimetic assembly and activation of [FeFe]-hydrogenases. *Nature* **499**: 66–69.
- Birrell, J.A., Wrede, K., Pawlak, K., Rodriguez-Macii, P., Rüdiger, O., Reijerse, E.J., and Lubitz, W. (2016) Artificial maturation of the highly active heterodimeric [FeFe] hydrogenase from *Desulfovibrio desulfuricans* ATCC 7757. *Isr J Chem* **56**: 852–863.
- Blahut, M., Sanchez, E., Fisher, C.E., and Outten, F.W. (2020) Fe-S cluster biogenesis by the bacterial Suf pathway. *Biochim Biophys Acta Mol Cell Res* **1867**: 118829.
- Bölter, B. (2018) En route into chloroplasts: preproteins' way home. *Photosynth Res* **138**: 263–275.
- Britt, R.D., Rai, G., and Tao, L. (2020) Biosynthesis of the catalytic H-cluster of [FeFe] hydrogenase: the roles of the Fe-S maturase proteins HydE, HydF, and HydG. *Chem Sci* **11**: 10313–10323.
- Burton, N.A., Padilla, R.V., Rose, A., and Habibullah, H. (2021) Increasing the efficiency of hydrogen production from solar powered water electrolysis. *Renew Sustain Energy Rev* **135**: 110255.
- Caserta, G., Adamska-Venkatesh, A., Pecqueur, L., Atta, M., Artero, V., Roy, S., *et al.* (2016) Chemical assembly of multiple metal cofactors: the heterologously expressed multidomain [FeFe]-hydrogenase from *Megasphaera elsdenii*. *Biochim Biophys Acta Bioenerg* **1856**: 1734–1740.
- Castruita, M., Casero, D., Karpowicz, S.J., Kropat, J., Vieler, A., Hsieh, S.I., *et al.* (2011) Systems biology approach in *Chlamydomonas* reveals connections between copper nutrition and multiple metabolic steps. *Plant Cell* **23**: 1273–1292.
- Chochois, V., Dauvillee, D., Beyly, A., Tolleter, D., Cuine, S., Timpano, H., *et al.* (2009) Hydrogen production in *Chlamydomonas*: photosystem II-dependent and -independent pathways differ in their requirement for starch metabolism. *Plant Physiol* **151**: 631–640.
- Chongdar, N., Birrell, J.A., Pawlak, K., Sommer, C., Reijerse, E.J., Rüdiger, O., *et al.* (2018) Unique spectroscopic properties of the h-cluster in a putative sensory [FeFe] hydrogenase. *J Am Chem Soc* **140**: 1057–1068.
- Cournac, L., Mus, F., Bernard, L., Guedeney, G., Vignais, P., and Peltier, G. (2002) Limiting steps of hydrogen production in *Chlamydomonas reinhardtii* and *Synechocystis* PCC 6803 as analysed by light-induced gas exchange transients. *Int J Hydrog Energy* **27**: 1229–1237.
- Cracknell, J.A., Wait, A.F., Lenz, O., Friedrich, B., and Armstrong, F.A. (2009) A kinetic and thermodynamic understanding of O<sub>2</sub> tolerance in [NiFe]-hydrogenases. *Proc Natl Acad Sci USA* **106**: 20681–20686.
- Crozet, P., Navarro, F.J., Willmund, F., Mehrshahi, P., Bakowski, K., Lauersen, K.J., *et al.* (2018) Birth of a photosynthetic chassis: a MoClo toolkit enabling synthetic biology in the microalga *Chlamydomonas reinhardtii*. *ACS Synth Biol* **7**: 2074–2086.
- Dai, Y., and Outten, F.W. (2012) The *E. coli* SufS - SufE sulfur transfer system is more resistant to oxidative stress than IscS - IscU. *FEBS Lett* **16**: 4016–4022.
- Diakonova, A.N., Khrushchev, S.S., Kovalenko, I.B., Riznichenko, G.Y., and Rubin, A.B. (2016) Influence of pH and ionic strength on electrostatic properties of ferredoxin, FNR, and hydrogenase and the rate constants of their interaction. *Phys Biol* **13**: 0506004.
- Dickson, D.J., Page, C.J., and Ely, R.L. (2009) Photobiological hydrogen production from *Synechocystis* sp. PCC 6803 encapsulated in silica sol-gel. *Int J Hydrog Energy* **34**: 204–215.
- Dinis, P., Suess, D.L.M., Fox, S.J., Harmer, J.E., Driesener, R.C., De La Paz, L., *et al.* (2015) X-ray crystallographic and EPR spectroscopic analysis of HydG, a maturase in [FeFe]-hydrogenase H-cluster assembly. *Proc Natl Acad Sci USA* **112**: 1362–1367.
- Driesener, R.C., Challand, M.R., McGlynn, S.E., Shepard, E.M., Boyd, E.S., Broderick, J.B., *et al.* (2010) [FeFe]-



- hydrogenase cyanide ligands derived from S-adenosylmethionine-dependent cleavage of tyrosine. *Angew Chem Int Ed* **49**: 1687–1690.
- Eilenberg, H., Weiner, I., Ben-Zvi, O., Pundak, C., Marmari, A., Liran, O., *et al.* (2016) The dual effect of a ferredoxin-hydrogenase fusion protein *in vivo*: successful divergence of the photosynthetic electron flux towards hydrogen production and elevated oxygen tolerance. *Biotechnol Biofuels* **9**: 1–10.
- Elman, T., Schweitzer, S., Shahar, N., Swartz, J., and Yacoby, I. (2020) Engineered clostridial [FeFe]-hydrogenase shows improved O<sub>2</sub> tolerance in *Chlamydomonas reinhardtii*. *Int J Hydrog Energy* **45**: 30201–30210.
- Esselborn, J., Lambert, C., Adamska-Venkatesh, A., Simmons, T., Berggren, G., Noth, J., *et al.* (2013) Spontaneous activation of [FeFe]-hydrogenases by an inorganic [2Fe] active site mimic. *Nat Chem Biol* **9**: 607–609.
- Esselborn, J., Muraki, N., Klein, K., Engelbrecht, V., Metzler-Nolte, N., Apfel, U.-P., *et al.* (2016) A structural view of synthetic cofactor integration into [FeFe]-hydrogenases. *Chem Sci* **7**: 959–968.
- Fabris, M., Abbriano, R.M., Pernice, M., Sutherland, D.L., Commault, A.S., Hall, C.C., *et al.* (2020) Emerging technologies in algal biotechnology: toward the establishment of a sustainable, algae-based bioeconomy. *Frontiers in Plant Science* **11**: 279.
- Fakhimi, N., Gonzalez-Ballester, D., Fernández, E., Galván, A., and Dubini, A. (2020) Algae-bacteria consortia as a strategy to enhance H<sub>2</sub> production. *Cells* **9**: 1353.
- Fei, X., and Deng, X. (2007) A novel Fe deficiency-responsive element (FeRE) regulates the expression of *atx1* in *Chlamydomonas reinhardtii*. *Plant Cell Physiol* **48**: 1496–1503.
- Fischer, N., and Rochaix, J.-D. (2001) The flanking regions of *PsaD* drive efficient gene expression in the nucleus of the green alga *Chlamydomonas reinhardtii*. *Mol Genet Genom* **265**: 888–894.
- Forestier, M., King, P., Zhang, L., Posewitz, M., Schwarzer, S., Happe, T., *et al.* (2003) Expression of two [Fe]-hydrogenases in *Chlamydomonas reinhardtii* under anaerobic conditions. *Eur J Biochem* **270**: 2750–2758.
- Fouchard, S., Hemschemeier, A., Caruana, A., Pruvost, J., Legrand, J., Happe, T., *et al.* (2005) Autotrophic and mixotrophic hydrogen photoproduction in sulfur-deprived *Chlamydomonas* cells. *Appl Environ Microbiol* **71**: 6199–6205.
- Ghirardi, M.L. (2015) Implementation of photobiological H<sub>2</sub> production: the O<sub>2</sub> sensitivity of hydrogenases. *Photosynth Res* **152**: 383–393.
- Ghysels, B., Godaux, D., Matagne, R.F., Cardol, P., and Franck, F. (2013) Function of the chloroplast hydrogenase in the microalga *Chlamydomonas*: the role of hydrogenase and state transitions during photosynthetic activation in anaerobiosis. *PLoS One* **8**: e64161.
- Gimpel, J.A., Hyun, J.S., Schoepp, N.G., and Mayfield, S.P. (2015) Production of recombinant proteins in microalgae at pilot greenhouse scale. *Biotechnol Bioeng* **112**: 339–345.
- Godaux, D., Bailleul, B., Berne, N., and Cardol, P. (2015) Induction of photosynthetic carbon fixation in anoxia relies on hydrogenase activity and proton-gradient regulation-Like1-mediated cyclic electron flow in *Chlamydomonas reinhardtii*. *Plant Physiol* **168**: 648–658.
- Godman, J., and Balk, J. (2008) Genome analysis of *Chlamydomonas reinhardtii* reveals the existence of multiple, compartmentalized iron-sulfur protein assembly machineries of different evolutionary origins. *Genetics* **179** (1): 59–68.
- Godman, J.E., Molnár, A., Baulcomb, D.C., and Balk, J. (2010) RNA silencing of hydrogenase(-like) genes and investigation of their physiological roles in the green alga *Chlamydomonas reinhardtii*. *Biochem J* **431**: 345–351.
- Gomez-Casati, D.F., Busi, M.V., Barchiesi, J., Pagani, M.A., Marchetti-Acosta, N.S., and Terenzi, A. (2021) Fe-S protein synthesis in green algae mitochondria. *Plants* **10**: 200.
- Gonzalez-Ballester, D., Casero, D., Cokus, S., Pellegrini, M., Merchant, S.S., and Grossman, A.R. (2010) RNA-Seq analysis of sulfur-deprived *Chlamydomonas* cells reveals aspects of acclimation critical for cell survival. *Plant Cell* **22**: 2058–2084.
- Greiner, A., Kelterborn, S., Evers, H., Kreimer, G., Sizova, I., and Hegemann, P. (2017) Targeting of photoreceptor genes in *Chlamydomonas reinhardtii* via zinc-finger nucleases and CRISPR/Cas9. *Plant Cell* **29**: 2498–2518.
- Gutekunst, K., Hoffmann, D., Westernströer, U., Schulz, R., Garbe-Schönberg, D., and Appel, J. (2018) In-vivo turnover frequency of the cyanobacterial NiFe-hydrogenase during photohydrogen production outperforms in-vitro systems. *Sci Rep* **8**(1): 6083.
- Guzmán-Zapata, D., Sandoval-Vargas, J., Macedo-Osorio, K., Salgado-Manjarrez, E., Castrejón-Flores, J., Oliver-Salvador, M., *et al.* (2019) Efficient editing of the nuclear APT reporter gene in *Chlamydomonas reinhardtii* via expression of a CRISPR-Cas9 module. *Int J Mol Sci* **20**: 1247.
- Happe, T., Mosler, B., and Naber, J.D. (1994) Induction, localization and metal content of hydrogenase in the green alga *Chlamydomonas reinhardtii*. *Eur J Biochem* **222**: 769–774.
- Happe, T., and Naber, J.D. (1993) Isolation, characterization and N-terminal amino acid sequence of hydrogenase from the green alga *Chlamydomonas reinhardtii*. *Eur J Biochem* **214**: 475–481.
- Hemschemeier, A., and Happe, T. (2011) Alternative photosynthetic electron transport pathways during anaerobiosis in the green alga *Chlamydomonas reinhardtii*. *Biochim Biophys Acta Bioenerg* **1807**: 919–926.
- Hertle, A.P., Blunder, T., Wunder, T., Pesaresi, P., Pribil, M., Armbruster, U., and Leister, D. (2013) PGRL1 is the elusive ferredoxin-plastoquinone reductase in photosynthetic cyclic electron flow. *Mol Cell* **49**: 511–523.
- IEA (2019) *The Future of Hydrogen*. Paris: IEA. URL <https://www.iea.org/reports/the-future-of-hydrogen>
- Jagadevan, S., Banerjee, A., Banerjee, C., Guria, C., Tiwari, R., Baweja, M., and Shukla, P. (2018) Recent developments in synthetic biology and metabolic engineering in microalgae towards biofuel production. *Biotechnol Biofuels* **11**: 185.
- Johnson, X., Steinbeck, J., Dent, R.M., Takahashi, H., Richaud, P., Ozawa, S.-I., *et al.* (2014) Proton gradient

- regulation 5-mediated cyclic electron flow under ATP- or redox-limited conditions: a study of  $\Delta$ ATPase pgr5 and  $\Delta$ rbcL pgr5 mutants in the green alga *Chlamydomonas reinhardtii*. *Plant Physiol* **165**: 438–452.
- Kanygin, A., Milrad, Y., Thummala, C., Reifschneider, K., Baker, P., Marco, P., *et al.* (2020) Rewiring photosynthesis: a photosystem I-hydrogenase chimera that makes H<sub>2</sub> *in vivo*. *Energy Environ Sci* **13**(9): 2903–2914.
- Kertess, L., Adamska-Venkatesh, A., Rodríguez-Maciá, P., Rudiger, O., Lubitz, W., and Happe, T. (2017) Influence of the [4Fe–4S] cluster coordinating cysteines on active site maturation and catalytic properties of *C. reinhardtii* [FeFe]-hydrogenase. *Chem Sci* **8**: 8127–8137.
- Koo, J., Schnabel, T., Liang, S., Evitt, N.H., and Swartz, J.R. (2017) High-throughput screening of catalytic H<sub>2</sub> production. *Angew Chem Int Ed* **56**: 1012–1016.
- Koo, J., and Swartz, J.R. (2018) System analysis and improved [FeFe] hydrogenase O<sub>2</sub> tolerance suggest feasibility for photosynthetic H<sub>2</sub> production. *Metab Eng* **49**: 21–27.
- Kosourov, S., Jokel, M., Aro, E.-M., and Allahverdiyeva, Y. (2018) A new approach for sustained and efficient H<sub>2</sub> photoproduction by *Chlamydomonas reinhardtii*. *Energy Environ Sci* **11**: 1431–1436.
- Kosourov, S., Nagy, V., Shevela, D., Jokel, M., Messinger, J., and Allahverdiyev, Y. (2020) Water oxidation by photosystem II is the primary source of electrons for sustained H<sub>2</sub> photoproduction in nutrient-replete green algae. *Proc Natl Acad Sci USA* **117**: 29629–29636.
- Kosourov, S., Seibert, M., and Ghirardi, M.L. (2003) Effects of extracellular pH on the metabolic pathways in sulfur-deprived, H<sub>2</sub>-producing *Chlamydomonas reinhardtii* cultures. *Plant Cell Physiol* **44**: 146–155.
- Kruse, O., Rupprecht, J., Bader, K.-P., Thomas-Hall, S., Schenk, P.M., Finazzi, G., and Hankamer, B. (2005) Improved photobiological H<sub>2</sub> production in engineered green algal cells. *J Biol Chem* **280**: 34170–34177.
- Land, H., Ceccaldi, P., Meszaros, L.S., Lorenzi, M., Redman, H.J., Senger, M., *et al.* (2019) Discovery of novel [FeFe]-hydrogenases for biocatalytic H<sub>2</sub>-production. *Chem Sci* **10**: 9941–9948.
- Land, H., Senger, M., Berggren, G., and Stripp, S.T. (2020) Current state of [FeFe]-hydrogenase research: biodiversity and spectroscopic investigations. *ACS Catal* **10**: 7069–7086.
- Lauersen, K.J., Kruse, O., and Mussgnug, J.H. (2015) Targeted expression of nuclear transgenes in *Chlamydomonas reinhardtii* with a versatile, modular vector toolkit. *Appl Microbiol Biotechnol* **99**: 3491–3503.
- Ley, M.B., Jepsen, L.H., Lee, Y.-S., Cho, Y.W., Bellosta von Colbe, J.M., Dornheim, M., *et al.* (2014) Complex hydrides for hydrogen storage – new perspectives. *Mater Today* **17**: 122–128.
- Liran, O., Semyatich, R., Milrad, Y., Eilenberg, H., Weiner, I., and Yacoby, I. (2016) Microoxic niches within the thylakoid stroma of air-grown *Chlamydomonas reinhardtii* protect [FeFe]-hydrogenase and support hydrogen production under fully aerobic environment. *Plant Physiol* **172**: 264–271.
- Lukey, M.J., Roessler, M.M., Parkin, A., Evans, R.M., Davies, R.A., Lenz, O., *et al.* (2011) Oxygen-tolerant [NiFe]-hydrogenases: the individual and collective importance of supernumerary cysteines at the proximal Fe-S cluster. *J Am Chem Soc* **133**: 16881–16892.
- Madden, C., Vaughn, M.D., Díez-Pérez, I., Brown, K.A., King, P.W., Gust, D., *et al.* (2012) Catalytic turnover of [FeFe]-hydrogenase based on single-molecule imaging. *J Am Chem Soc* **134**: 1577–1582.
- Melis, A., Zhang, L., Forestier, M., Ghirardi, M.L., and Seibert, M. (2000) Sustained photobiological hydrogen gas production upon reversible inactivation of oxygen evolution in the green alga *Chlamydomonas reinhardtii*. *Plant Physiol* **122**: 127–135.
- Meuser, J.E., D'Adamo, S., Jinkerson, R.E., Mus, F., Yang, W., Ghirardi, M.L., *et al.* (2012) Genetic disruption of both *Chlamydomonas reinhardtii* [FeFe]-hydrogenases: Insight into the role of HYDA2 in H<sub>2</sub> production. *Biochem Biophys Res Commun* **417**: 704–709.
- Milrad, Y., Schweitzer, S., Feldman, Y., and Yacoby, I. (2018) Green algal hydrogenase activity is outcompeted by carbon fixation before inactivation by oxygen takes place. *Plant Physiol* **177**: 918–926.
- Mišlov, D., Cifrek, M., Krois, I., and Džapo, H. (2015) Measurement of dissolved hydrogen concentration with Clark electrode, 2015 IEEE Sensors Applications Symposium (SAS): 1–5.
- Mulder, D.W., Boyd, E.S., Sarma, R., Lange, R.K., Endrizzi, J.A., Broderick, J.B., and Peters, J.W. (2010) Stepwise [FeFe]-hydrogenase H-cluster assembly revealed in the structure of HydA<sup>ΔEFG</sup>. *Nature* **465**: 248–252.
- Mulder, D.W., Guo, Y., Ratzloff, M.W., and King, P.W. (2017) Identification of a catalytic iron-hydride at the H-Cluster of [FeFe]-hydrogenase. *J Am Chem Soc* **139**: 83–86.
- Mulder, D.W., Ortillo, D.O., Gardenghi, D.J., Naumov, A.V., Ruebush, S.S., Szilagy, R.K., *et al.* (2009) Activation of HydA<sup>ΔEFG</sup> requires a preformed [4Fe-4S] cluster. *Biochemistry* **48**: 6240–6248.
- Mus, F., Cournac, L., Cardellini, V., Caruana, A., and Peltier, G. (2005) Inhibitor studies on non-photochemical plastoquinone reduction and H<sub>2</sub> photoproduction in *Chlamydomonas reinhardtii*. *Biochim Biophys Acta Bioenerg* **1708**: 322–332.
- Nagy, V., Vidal-Meireles, A., Podmaniczki, A., Szentmihályi, K., Rakhely, G., Zsigmond, L., *et al.* (2018) The mechanism of photosystem-II inactivation during sulphur deprivation-induced H<sub>2</sub> production in *Chlamydomonas reinhardtii*. *Plant J* **94**: 548–561.
- Nakahira, Y., Ogawa, A., Asano, H., Oyama, T., and Tozawa, Y. (2013) Theophylline-dependent riboswitch as a novel genetic tool for strict regulation of protein expression in cyanobacterium *Synechococcus elongatus* PCC 7942. *Plant Cell Physiol* **54**: 1724–1735.
- Ng, I.-S., Keskin, B.B., and Tan, S.-I. (2020) A critical review of genome editing and synthetic biology applications in metabolic engineering of microalgae and cyanobacteria. *Biotechnol J* **15**: 1900228.
- Nicolet, Y. (2019) How [Fe]-hydrogenase metabolizes dihydrogen. *Nat Catal* **2**: 481–482.
- Nikolova, D., Heilmann, C., Hawat, S., Gäbelein, P., and Hippler, M. (2018) Absolute quantification of selected photosynthetic electron transfer proteins in *Chlamydomonas*

- reinhardtii* in the presence and absence of oxygen. *Photosynth Res* **137**: 281–293.
- Noone, S., Ratcliff, K., Davis, R.A., Subramanian, V., Meuser, J., Posewitz, M.C., *et al.* (2017) Expression of a clostridial [FeFe]-hydrogenase in *Chlamydomonas reinhardtii* prolongs photo-production of hydrogen from water splitting. *Algal Res* **22**: 116–121.
- Noth, J., Krawietz, D., Hemschemeir, A., and Happe, T. (2013) Pyruvate ferredoxin oxidoreductase is coupled to light-independent hydrogen production in *Chlamydomonas reinhardtii*. *J Biol Chem* **288**: 4368–4377.
- Outten, F.W., Wood, M.J., Munoz, F.M., and Storz, G. (2003) The SufE protein and the SufBCD complex enhance sulfs cysteine desulfurase activity as part of a sulfur transfer pathway for Fe-S cluster assembly in *Escherichia coli*. *J Biol Chem* **278**: 45713–45719.
- Paila, Y.D., Richardson, L.G.L., and Schnell, D.J. (2015) New insights into the mechanism of chloroplast protein import and its integration with protein quality control, organelle biogenesis and development. *J Mol Biol* **13**: 1038–1060.
- Pape, M., Lambert, C., Happe, T., and Hemschemeir, A. (2012) Differential expression of the *Chlamydomonas* [FeFe]-hydrogenase-encoding HYDA1 gene is regulated by the copper response regulator1. *Plant Physiol* **159**: 1700–1712.
- Pelmenschikov, V., Birrell, J.A., Pham, C.C., Mishra, N., Wang, H., Sommer, C., *et al.* (2017) Reaction coordinate leading to H<sub>2</sub> production in [FeFe]-hydrogenase identified by nuclear resonance vibrational spectroscopy and density functional theory. *J Am Chem Soc* **139**: 16894–16902.
- Pérard, J., and Ollagnier de Choudens, S. (2018) Iron–sulfur clusters biogenesis by the SUF machinery: close to the molecular mechanism understanding. *J Biol Inorg Chem* **23**: 581–596.
- Peters, J.W., Schut, G.J., Boyd, E.S., Mulder, D.W., Shepard, E.M., Broderick, J.B., *et al.* (2015) [FeFe]- and [NiFe]-hydrogenase diversity, mechanism, and maturation. *Biochim Biophys Acta Mol Cell Res* **1853**: 1350–1369.
- Petrova, E.V., Kukarskikh, G.P., Krendeleva, T.E., and Antal, K. (2020) The mechanisms and role of photosynthetic hydrogen production by green microalgae. *Microbiology* **89**: 251–265.
- Polle, J.E.W., Benemann, J.R., Tanaka, A., and Melis, A. (2000) Photosynthetic apparatus organization and function in the wild type and a chlorophyll b-less mutant of *Chlamydomonas reinhardtii*. dependence on carbon source. *Planta* **211**: 335–344.
- Posewitz, M.C., King, P.W., Smolinski, S.L., Zhang, L., Seibert, M., and Ghirardi, M.L. (2004a) Discovery of two novel radical S-adenosylmethionine proteins required for the assembly of an active [Fe] hydrogenase. *J Biol Chem* **24**: 25711–25720.
- Posewitz, M.C., Smolinski, S.L., Kanakagiri, S., Melis, A., Seibert, M., and Ghirardi, M.L. (2004b) Hydrogen photo-production is attenuated by disruption of an isoamylase gene in *Chlamydomonas reinhardtii*. *Plant Cell* **16**: 2151–2163.
- Ramachandran, R., and Menon, R.K. (1998) An overview of industrial uses of hydrogen. *Int J Hydrog Energy* **23**: 593–598.
- Rao, G., Tao, L., and Britt, R.D. (2020) Serine is the molecular source of the NH(CH<sub>2</sub>)<sub>2</sub> bridgehead moiety of the in vitro assembled [FeFe] hydrogenase H-cluster. *Chem Sci* **11**: 1241–1247.
- Reifschneider-Wegner, K., Kanygin, A., and Redding, K.E. (2014) Expression of the [FeFe] hydrogenase in the chloroplast of *Chlamydomonas reinhardtii*. *Int J Hydrog Energy* **39**: 3657–3665.
- Reijerse, E.J., Pham, C.C., Pelmenschikov, V., Gilbert-Wilson, R., Adamska-Venkatesh, A., Siebel, J.F., *et al.* (2017) Direct observation of an iron-bound terminal hydride in [FeFe]-hydrogenase by nuclear resonance vibrational spectroscopy. *J Am Chem Soc* **139**: 4306–4309.
- Rodríguez-Macia, P., Breuer, N., DeBeer, S., and Birrell, J.A. (2020) Insight into the redox behavior of the [4Fe–4S] subcluster in [FeFe] hydrogenases. *ACS Catal* **10**: 13084–13095.
- Rumpel, S., Siebel, J.F., Farès, C., Duan, J., Reijerse, E., Happe, T., *et al.* (2014) Enhancing hydrogen production of microalgae by redirecting electrons from photosystem I to hydrogenase. *Energy Environ Sci* **7**: 3296–3301.
- Salomé, P.A., and Merchant, S.S. (2019) A series of fortunate events: introducing *Chlamydomonas* as a reference organism. *Plant Cell* **31**: 1682–1707.
- Sasso, S., Stibor, H., Mittag, M., and Grossman, A.R. (2018) From molecular manipulation of domesticated *Chlamydomonas reinhardtii* to survival in nature. *eLife* **7**: e39233. doi: 10.7554/eLife.39233.001
- Sawyer, A., Bai, Y., Lu, Y., Hemschemeir, A., and Happe, T. (2017) Compartmentalisation of [FeFe]-hydrogenase maturation in *Chlamydomonas reinhardtii*. *Plant J* **90**: 1134–1143.
- Sawyer, A., and Winkler, M. (2017) Evolution of *Chlamydomonas reinhardtii* ferredoxins and their interactions with [FeFe]-hydrogenases. *Photosynth Res* **134**: 307–316.
- Schrader, P.S., Burrows, E.H., and Ely, R.L. (2008) High-throughput screening assay for biological hydrogen production. *Anal Chem* **80**: 4014–4019.
- Scranton, M.A., Ostrand, J.T., Georgianna, D.R., Lofgren, S.M., Li, D., Ellis, R.C., *et al.* (2016) Synthetic promoters capable of driving robust nuclear gene expression in the green alga *Chlamydomonas reinhardtii*. *Algal Res* **15**: 135–142.
- Selbach, B.P., Pradhan, P.K., and Santos, P.C.D. (2013) Protected sulfur transfer reactions by the *Escherichia coli* suf system. *Biochemistry* **52**: 4089–4096.
- Shepard, E.M., Duffus, B.R., George, S.J., McGlynn, S.E., Challand, M.R., Swanson, K.D., *et al.* (2010) [FeFe]-hydrogenase maturation: HydG-catalyzed synthesis of carbon monoxide. *J Am Chem Soc* **132**: 9247–9249.
- Shin, M. (2004) How is ferredoxin-NADP reductase involved in the NADP photoreduction of chloroplasts? *Photosynth Res* **80**: 307–313.
- Shin, S.-E., Lim, J.-M., Koh, H., Kim, E.K., Kang, N.K., Jeon, S., *et al.* (2016) (2016) CRISPR/Cas9-induced knockout and knock-in mutations in *Chlamydomonas reinhardtii*. *Sci Rep* **6**: 27810.
- Seibert, M., Benson, D.K., and Flynn, T.M. (2001) *Method and Apparatus for Rapid Biohydrogen Phenotypic Screening of Microorganisms Using a Chemochromic Sensor.*

- U.S. patent 6,277,589 B1. Kansas City, MO: Midwest Research Institute.
- Søndergaard, D., Pedersen, C.N.S., and Greening, C. (2016) HydDB: a web tool for hydrogenase classification and analysis. *Sci Rep* **6**: 34212–34220.
- Srirangan, K., Pyne, M.E., and Chou, C.P. (2011) Biochemical and genetic engineering strategies to enhance hydrogen production in photosynthetic algae and cyanobacteria. *Bioresour Technol* **102**: 8589–8604.
- Stapleton, J.A., and Swartz, J.R. (2010a) A cell-free microtiter plate screen for improved [FeFe] hydrogenases. *PLoS One* **5**: 1–8.
- Stapleton, J.A., and Swartz, J.R. (2010b) Development of an *in vitro* compartmentalization screen for high-throughput directed evolution of [FeFe] hydrogenases. *PLoS One* **5**: e15275.
- Steinbeck, J., Nikolova, D., Weingarten, R., Johnson, X., Richaud, P., Peltier, G., *et al.* (2015) Deletion of Proton Gradient Regulation 5 (PGR5) and PGR5-Like 1 (PGRL1) proteins promote sustainable light-driven hydrogen production in *Chlamydomonas reinhardtii* due to increased PSII activity under sulfur deprivation. *Front Plant Sci* **6**: 892.
- Strenkert, D., Schmollinger, S., Gallaher, S.D., Salomé, P.A., Purvine, S.O., Nicora, C.D., *et al.* (2019) Multiomics resolution of molecular events during a day in the life of *Chlamydomonas*. *Proc Natl Acad Sci USA* **116**: 2374–2383.
- Suess, D.L.M., Bürstel, I., De La Paz, L., Kuchenreuther, J.M., Pham, C.C., Cramer, S.P., *et al.* (2015) Cysteine as a ligand platform in the biosynthesis of the FeFe hydrogenase H cluster. *Proc Natl Acad Sci USA* **112**: 11455–11460.
- Surzycki, R., Cournac, L., Peltier, G., and Rochaix, J.-D. (2007) Potential for hydrogen production with inducible chloroplast gene expression in *Chlamydomonas*. *Proc Natl Acad Sci USA* **104**: 17548–17553.
- Swanson, K.D., Ratzloff, M.W., Mulder, D.W., Artz, J.H., Ghose, S., Hoffman, A., *et al.* (2015) [FeFe]-hydrogenase oxygen inactivation is initiated at the H cluster 2Fe sub-cluster. *J Am Chem Soc* **137**: 1809–1816.
- Takabayashi, A., Kishine, M., Asada, K., Endo, T., and Sato, F. (2005) Differential use of two cyclic electron flows around photosystem I for driving CO<sub>2</sub>-concentration mechanism in C<sub>4</sub> photosynthesis. *Proc Natl Acad Sci USA* **102**: 16898–16903.
- Takahashi, Y., and Tokumoto, U. (2002) A third bacterial system for the assembly of iron-sulfur clusters with homologs in archaea and plastids. *J Biol Chem* **277**: 28380–28383.
- Tao, L., Pattenaude, S.A., Joshi, S., Begley, T.P., Rauffuss, T.B., and Britt, R.D. (2020) Radical SAM enzyme hyde generates adenosylated Fe(I) intermediates En route to the [FeFe]-hydrogenase catalytic H-Cluster. *J Am Chem Soc* **142**: 10841–10848.
- Tolleter, D., Ghysels, B., Alric, J., Petroustos, D., Tolstygina, I., Krawietz, D., *et al.* (2011) Control of hydrogen photoproduction by the proton gradient generated by cyclic electron flow in *Chlamydomonas reinhardtii*. *Plant Cell* **23**: 2619–2630.
- Volgusheva, A., Kukarskikh, G., Krendeleva, T., Rubin, A., and Mamedov, F. (2015) Hydrogen photoproduction in green algae *Chlamydomonas reinhardtii* under magnesium deprivation. *RSC Adv* **5**: 5633–5637.
- Wecker, M.S.A., and Ghirardi, M.L. (2014) High-throughput biosensor discriminates between different algal H<sub>2</sub>-photoproducing strains. *Biotechnol Bioeng* **111**: 1332–1340.
- Wecker, M.S.A., Meuser, J.E., Posewitz, M.C., and Ghirardi, M.L. (2011) Design of a new biosensor for algal H<sub>2</sub> production based on the H<sub>2</sub>-sensing system of *Rhodobacter capsulatus*. *Int J Hydrog Energy* **36**: 11229–11237.
- Weijun, Y. (2015) Analytical accuracy of hydrogen measurement using gas chromatography with thermal conductivity detection. *J. Sep. Science* **38**: 2640–2646.
- Wichmann, J., Lauersen, K.J., and Kruse, O. (2020) Green algal hydrocarbon metabolism is an exceptional source of sustainable chemicals. *Curr Opin Biotechnol* **61**: 28–37.
- Wiegand, K., Winkler, M., Rumpel, S., Kannchen, D., Rexroth, S., Hase, T., *et al.* (2018) Rational redesign of the ferredoxin-NADP<sup>+</sup>-oxido-reductase/ferredoxin-interaction for photosynthesis-dependent H<sub>2</sub>-production. *Biochim Biophys Acta Bioenerg* **1859**: 253–262.
- Winkler, M., Duan, J., Rutz, A., Felbek, C., Scholtyssek, L., Lampret, O., *et al.* (2021) A safety cap protects hydrogenase from oxygen attack. *Nat Commun* **12**(1): 756.
- Wu, B., Matian, M., and Offer, G.J. (2012) Hydrogen PEMFC system for automotive applications. *Int J Low-Carbon Technol* **7**: 28–37.
- Xu, X.M., and Møller, S.G. (2011) Iron-sulfur clusters: Biogenesis, molecular mechanisms, and their functional significance. *Antioxid Redox Signal* **15**: 271–307.
- Yacoby, I., Pochekailov, S., Toporik, H., Ghirardi, M.L., King, P.W., and Zhang, S. (2011) Photosynthetic electron partitioning between [FeFe]-hydrogenase and ferredoxin: NADP<sup>+</sup>-oxidoreductase (FNR) enzymes *in vitro*. *Proc Natl Acad Sci USA* **108**: 9396–9401.
- Zanetti, G., and Pandini, V. (2013) Ferredoxin. In *Encyclopedia of Biological Chemistry*. Lennarz, W.J., and Lane, M.D. (eds). Cambridge, MA: Academic Press, pp. 296–298.